University of Nevada, Reno

Characterization and Assessment of Tensile Behavior of Carbon Nanofibers Enhanced Ultra-High Performance Concrete

A thesis submitted in partial fulfillment of the
requirements for the degree of Master of Science in
Civil and Environmental Engineering

by

Mohamed Ayman Hussein Hosny

Dr. Mohamed A. Moustafa/Thesis Advisor

December 2022

We recommend that the thesis
prepared under our supervision by

Mohamed Ayman Hosny

entitled

**Characterization and Assessment of Tensile Behavior of
Carbon Nanofibers Enhanced Ultra-High Performance
Concrete**

be accepted in partial fulfillment of the
requirements for the degree of

Master of Science

Mohamed A. Moustafa
Advisor

Elnaz Seylabi
Committee Member

Mustafa Hadj-Nacer
Graduate School Representative

Markus Kemmelmeier, Ph.D., Dean
Graduate School

December, 2022

ABSTRACT

Second only to water, concrete is the world's most consumed material, not surprisingly, concrete contributes to around 8% of global carbon emissions (Gagg, 2014). This motivates researchers to advance in cementitious material and explore possible breakthroughs in an attempt to further improve and optimize the limited available resources. One recent breakthrough in cementitious materials is Ultra High-Performance Concrete (UHPC). UHPC is an advanced class of concrete and cementitious materials that exhibits high mechanical and durability performance. These properties are achievable using packing density theory which optimizes the gradation of granular materials. In other words, UHPC depends on enhanced microstructure, accompanied by a low water/cement ratio and fiber reinforcement to achieve superior overall performance and durability. UHPC typically consists of cement, silica fume, sand, and a fine supplementary material including -but not limited to- fly ash or slag cement. The robustness and popularity of UHPC in different fields has pushed the interest of stakeholders to explore the UHPC tensile capabilities and behaviors. Evidently, there has been a growth in UHPC tensile research. The literature lacks any set of extensive data with variable fiber dosage.

In this study, extensive data is examined and commented on. This study is examining a commercial material named CeEntek which consists of sand, cement, water, carbon nanofiber, and superplasticizer. This study's comprehensive goal is to assess and characterize the tensile behavior of a nanofiber enhanced UHPC.

Another goal of the study is to document the post-cracking tensile behavior of the material. It dictates the future usage of the material as there are two anticipated failure behaviors: failure after gradual strain hardening or failure after crack localization. The first behavior would provide warnings at peak loads which is favorable in general concrete elements design. With the variable fiber percentage in the experimental program, extensive data is generated helping in a better understanding of the tensile behavior of UHPC.

To achieve the mentioned goals, an experimental program was set. The experimental investigation consisted of tests on prims, cylinders, and dog-bone-shaped specimens with varying steel fiber content. Four-point bending, direct tension, and compression tests were carried out according to ASTM specifications and extensive data on their compressive, tensile, and flexural behavior were recorded and analyzed.

ACKNOWLEDGMENTS

All praise and thanks to Allah (God) for giving me the strength and the patience to complete this work.

I would not have completed this work without the support I received from my dear and close family and friends over the last year, to whom I am sincerely thankful.

I would like to express my gratitude to my advisor, Dr. Mohamed Moustafa. I am thankful for the opportunity to work within his team, his guidance and unshaken support during my program. I would also like to thank Dr. Elnaz Seylabi and Dr. Mustafa Hadj Nacer for being on my committee, their support and feedback.

I thank my family for their continuous support and prayers all time. That starts with my parents; my father Prof. Ayman Hussein who pushed me and supported me in all manner of ways, my mother for her unconditional love and support. I would also like to thank my sister Sara and my brother Abdel hady for their continuous encouragement and help.

I would like to thank Chad Lyttle and Todd Lyttle for their support and time in the laboratory. Also, I would also like to thank my friends during the time of the study for their support and encouragements. This includes Dr. Sherif Elfass, Mario Mendieta, Moaaz Hassan and Muhammed Khaled.

TABLE OF CONTENTS

LIST OF TABLES

LIST OF FIGURES

1. INTRODUCTION

1.1 Overview

In recent decades, efforts are set on high strength materials especially in structural engineering applications. Communities are more interested in lightweight, slender, and aesthetically pleasing members. With motivating reasons, researchers were keen to provide the industry with reliable and promising materials, which led them to developing a new material with better performance and durability than the traditional old concrete. In concrete research community the new material is known as ultra-high performance concrete. It is an advanced class of concrete and cementitious materials that exhibits high mechanical and durability properties (Graybeal et al., 2007). UHPC is characterized by the gradation of granular materials, low water to cement ratio, less than 0.25, which all attribute to the superiority of the material. The UHPC depends on having better microstructure by having less porosity and better homogeneity granting overall increased toughness (J. Li et al., 2020). One of the composition differences of UHPC from normal traditional concrete, is the absence of coarse aggregates. With that in mind and using the optimized gradation of the materials, we get a dense packed matrix of material with low permeability resulting in a ductile, durable, and reliable material. In favor of all mentioned above, UHPC exhibits high compressive strength exceeding 22 ksi, six times conventional concrete (Aboukifa, et al., 2020). With these merits of UHPC, it will still have a brittle failure pattern, which is not desirable in a general sense, yet with small content of fibers, it will shift from brittle failure to a ductile desirable pattern (Park et al., 2012).

Numerous research has developed the idea behind UHPC and new types of UHPC has come to surface. For example, eco-friendly UHPC-BC (belite cement) has lower environmental impact than UHPC-OPC (ordinary Portland cement) with having higher compressive and flexural strength than OPC only in 28 and 90 days (Li et al., 2022). Another research concludes that adding steel slag powder helps in improving workability and early strength without affecting any mechanical properties with the addition of having lower energy consumption and emissions compared to other options (Fan et al., 2021). One idea surfaced and gained a lot of attraction, adding nano materials to the mix of UHPC. One research effort investigated the behavior of nano metaclayed as an additive to UHPC (Norhasri et al., 2019). Nanomaterials can hugely affect positively the UHPC behavior (Safiuddin et al., 2014). In this study, a commercial proprietary nanofiber enhanced UHPC material from CeEntek which has been readily used across the United States is examined and investigated (CeEntek, website). The literature lacks data on nanofiber enhanced UHPC in tensile behavior which stimulates this study to examine the characteristics and assess the behavior of the nanofiber enhanced UHPC.

1.2 Background and literature

1.2.1 UHPC

The term "UHPC" stands for Ultra-High Performance Concrete, which is a relatively new class of cementitious composite materials. In broad terms, it can be classified as a cementitious composite characterized by high mechanical properties with less porosity and better homogeneity than traditional concrete. Typically, UHPC will utilize fiber reinforcement which will be mixed with other ingredients during initial mixing. UHPC is

designed using packing density theory, water content to cementitious material ratio less than 0.25, and an optimized gradation of granular materials. Unlike traditional concrete, UHPC does not have any coarse aggregate, combined with steel fiber and the mentioned characteristics, it achieves a high durability and high strength material (Haber et al., 2017.)

UHPC depends on the refined microstructure and fiber reinforcement to meet with the demand of high mechanical properties such as high compressive strength, post-cracking tensile strength and overall ductility. Usually UHPC consists of cementitious material, fine sand, supplementary materials, superplasticizer, water, and fiber (Akeed et al., 2022).

1.2.2 UHPC applications

The superiority of UHPC allows its use in numerous applications from small size connections and overlays to full structural components and members. Federal Highway administration (FHWA) has made immense efforts to implement the use of UHPC in bridge constructions, with the first UHPC prestressed I-girder bridge opened to traffic in 2006. Till now, over 377 bridges were constructed with UHPC, and between the 2020-2021 year over 100 bridges were built using UHPC (FHWA, website). UHPC becomes more convenient to use for accelerated construction, such as precast and prestressed bridges. Connections and overlays typically would be the last item on the project with the necessity to open the bridge for traffic as fast as possible (Figure 1.1). UHPC will have fast setting rate with the guarantee of meeting the design requirements in less time than traditional concrete. Recent studies showed the high potential of durability and ductility achievable with UHPC (Aboukifa, et al, 2021). On the structural components, more research efforts are exploring the behavior of UHPC in large scale, several studies at UNR among others

showed promising and adequate ductile behavior of axial, slender, and seismic columns subjected to combined axial and lateral loading (Joe and Moustafa 2016; Aboukifa et al. 2020; Aboukifa et al. 2021; Aboukifa and Moustafa 2021, 2022a, & 2022b). Commercial and non-proprietary UHPC was also used for bridge deck and other connections (Abokifa and Moustafa 2021a, 2021b, 2021c). UHPC also can be used in architectural façade, as it allows for slim and slender elements with avoiding cracks and breakage (hi-con, website). Furthermore, studies has developed detailed material and constitutive models for UHPC and finite element simulation (Naeimi and Moustafa 2020, 2021a, 2021b).
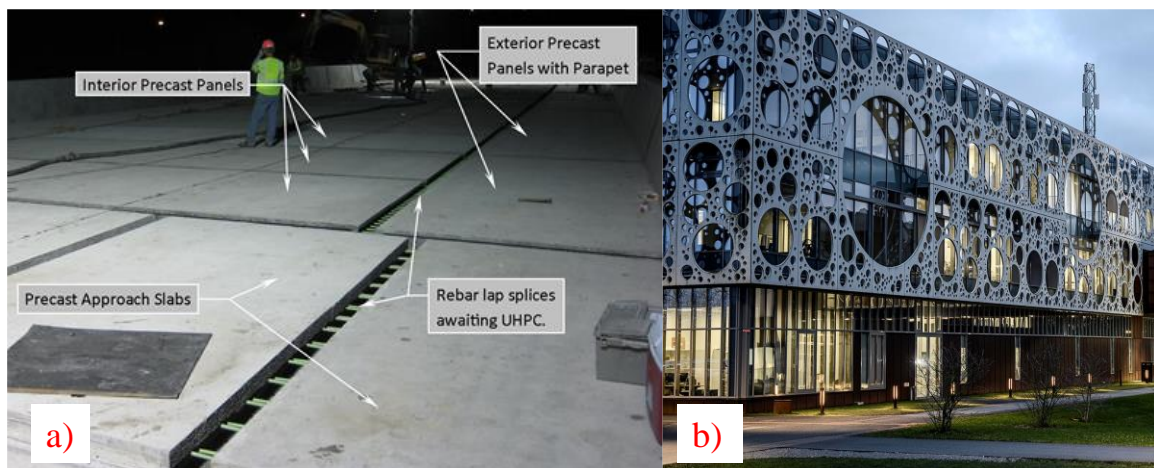
Figure 1-1 UHPC applications (a) Precast deck and connections (FHWA, Design and construction of field cast UHPC connections), (b) Architectural façade (hi-con website)

1.2.3 Recent trends in UHPC

UHPC is a class of concrete and cementitious material that can be mixed with different additives and technologies, from nanomaterials, recycled fibers to trying unorthodox materials such as glass. One research study explored the mechanical properties of eco-efficient UHPC with recycled tyre steel fibers and cords (Isa et al., 2021). Another research

study investigated the effects of reinforcement ratio, fiber orientation and chemical treating on tensile behavior (Qiu et al., 2020). A study examined the effects of adding nano-silica on UHPC (Yu et al., 2014). Nano metaclayed's effects were studied and found that strength development was seen at later ages (Norhasri et al., 2019). All of these are examples of how versatile UHPC is and how a lot of technologies and additives can be integrated with.

1.2.4   Carbon nanofibers enhanced concrete

Fibers are added to concrete or UHPC to help control the cracking and shift from a brittle sudden failure to a gradual ductile one. A step up from traditional fibers will be nanofibers as the theory behind it proposes it will delay the formation of cracks on the nano level unlike microfibers or microfibers, they delay the progress of macrocracks or microcracks respectively, but they do not stop their initiation. One study investigated the behavior of cement paste reinforced with carbon nanofibers, the research concluded the fibers were able to control the cracking on the nano level by bridging them and the pores in the cementitious matrix (Metaxa et al., 2010.). Another study evaluated the effects of carbon nanofibers and graphite nano platelets on UHPC. It was concluded that the use of nanomaterials reduced the total porosity of UHPC, while it did not contribute much to the yield stress (Meng & Khayat, 2018). Furthermore, a study examined the effects of using both nanomaterials and steel fibers on UHPC. It was concluded that nanomaterials and steel fibers are mainly responsible for matrix reinforcement, mitigating and controlling cracking, respectively (Huang et al., 2021). To add, another study investigated the effects of CNF on cement composites and found an increase in tensile strength up to 22% (Gay & Sanchez, 2010).

1.2.5   Tensile behavior of UHPC

In this subsection, utilized testing methods in literature are mentioned and discussed, also experimental programs of various studies are summarized. Direct tensile test is one of the most reliable and favored test where a specimen is pined between fixtures and a tensile force is applied either by a displacement rate or an incremental force rate. Specimens subjected to this test will be very sensitive to alignment and uneven surfaces as it may introduce bending moments or shear forces. Another test is flexural test which might be 3- or 4-point bending. A specimen of a prismatic shape typically 4 by 4 by 12 inches will be placed on 2 supports and either loaded by 1 point or 2 points hence the test is called 3- or 4-point bending test. The test is straight forward yet not a direct representation for tensile behavior as it incorporates some compression forces on the specimen's top section. Additionally, a splitting cylinder test is sometimes used. Splitting cylinder is a simple setup test, only requires a cylindrical specimen to be placed on its side and a load is applied till failure. It is not used often for UHPC as it does not capture the hardening behavior. Double punch test is another test that some studies implement which is also known as Barcelona test similar to splitting cylinder test with a different setup.

As research efforts advances and multiplies, the call for a standardized test that captures the tensile behavior has been repeatedly asked for. One of the challenges that was noticed in the literature study that each research might be using a different tensile test or maybe the same test but with different technique. Therefore, ASHTO proposed a 2 by 2 inch to be tested in direct tensile test as a base for comparison and future testing.

As for experimental programs, one study (Akça & İpek, 2022) investigated different fiber combinations and aimed to optimize of a nonproprietary mix of UHPC. They implemented flexural testing (3-point bending), splitting tensile test and pull-out test and compression test. They had various batches with 2 and 3% fiber percentages of straight and hook-end steel fibers. The researchers had two different curing methods: a water tank and a wet cloth. They tested prismatic specimens of size 3.93 by 3.93 by 15.74 inches (100 by 100 by 400 mm) for flexural tensile strength by four-point bending test, and prismatic specimens of size 1.96 by 1.96 by 11.81 inches (50 by 50 by 300 mm) were also tested for flexural tensile strength and cubic specimens of size 3.9 by 3.9 inches (100 by 100 mm) were tested for splitting tensile strength. Specimens were tested on the 28th day (Akça & İpek, 2022).

A study done by FHWA, had two different proprietary mixes of UHPC with 2 and 3% fiber percentages. A total of 5 batches was made, specimens were cured with steam or lab curing. The batches had varying specimens' sizes, for cylinders 3 inches (76 mm) 4.33 inches (110 mm) were test for compression mechanical properties: density, compressive, strength and modulus of elasticity. One of the UHPC mix had prismatic specimens with dimensions of 2 by 2 by 17 inches (50.8 by 50.8 by 431.8 mm) and 2 by 2 by 11 inches (50.8 by 50.8 by 279.4 mm), another batch had prismatic specimens 3.9 by 3.9 by 15.7 inches (100 by 100 by 400 mm). Specimens were tested roughly 4 months after casting (Graybeal & Baby, 2019).

 (Riding et al., 2022) had a nonproprietary mix of UHPC with straight and twisted steel fiber, their percentages of 1% to 3% with 0.5% increments resulting in 5 batches. The researchers had six beam specimens with dimensions of 2 by 2 by 17 inches (51 by 51 by

432 mm) for direct tension tests and four prismatic specimens with dimensions of 4 by 4 by 14 inches (102 by 102 by 356 mm). Double punch test was also used in this study by using three 6 by 6 inches (152 by 152 mm) cylindrical double punch specimens. The researchers did not mention how the specimens were cured. Last study, conducted by PCI, had flexural testing for 4 by 4 by 14-inch beams of different UHPC mixes, cured with product at 28 days and a criterion of acceptance was set for ductility and strength (Tadros et al., 2021).

1.2.6 Knowledge gaps

Considering all the mentioned information, there is clearly a lack of information on carbon nanofiber enhanced UHPC, and very limited data on tensile testing of specimens that, statistically, will be sufficient. That is the objective that this study has, as it aimed to generate a reliable amount of data of tensile testing.

1.3 Problem statement and Research objectives

As previously discussed, UHPC has superior mechanical properties and new variants are always emerging and revolutionized. Thus, research has to comprehensively explore and characterize the behavior of these materials to set the ground for industrial use, characterizing the materials will help in setting guidelines, criteria, standards, and codes for using the material in new design projects. Carbon nanofiber UHPC is a new mixture and literature is short on data on this type of UHPC, especially in tensile behavior characterization and comparison with traditional UHPC. In recent decades, nanomaterials gained the interest of researchers and how they affect the overall performance of

cementitious materials. Studies showed that using nanomaterials as a part of a concrete mixture can enhance the hardened properties, durability, and workability. CNF has the potential to bridge and bond the concrete mixture at the nano level, enhancing strength by having less permeability and tighter pores. Other studies showed addition of CNF has a positive impact on fluidity of UHPC, matrix reinforcement and better anti cracking behavior. To add, studies showed that CNF has enhanced overall behavior of concrete with the condition of well dispersion in the mix. Therefore, it is of a necessity to investigate and assess the tensile behavior of nanofiber enhanced UHPC to further serve the research community at large and provide a broad view of where research efforts should be focused on. The objective of this study is to be able to lay out an all-inclusive picture of nanofiber enhanced UHPC, to provide a better understanding for future research for tensile behavior. Another objective is to assess and compare the studied material with other materials available in the literature.

1.4 Methodology

Research work done in this study is sorely based on the extensive experimental program and the literature review, with some statistical and computational work. First, literature review focused on mechanical properties, characterization, and behavior of various UHPC. Second, experimental work started with three batches of CeEntek with different proportions to be tested in this study. Direct tension, 4-point bending, and compression testing was utilized to evaluate the UHPC behavior. Prismatic specimens of 3 by 3 by 12, ½ and 1 inch dog-bone specimens and cylinders of 3 by 6 inches were the main testing specimens. Third, computational and statistical work was conducted to assess the material.

1.5 Thesis Outline

This thesis is organized into five chapters: Introduction, Experimental program, Results and discussion, Assessment and trends, and Summary and conclusions. The introduction chapter gives a brief overview and explanation on UHPC, summaries the literature and provides an outline of the study. The experimental program goes through the testing program, mix proportions, specimens, testing techniques and explanations. The results and discussion lay out all results with some explanation and commentary. Assessment and trends will lay out the results of past literature side to side with this study's results. The final chapter provides overall outcomes, conclusions, and recommendations.

2. EXPERIMENTAL PROGRAM

The experimental investigation was carried out on cylinders, dog-bone shaped specimens and prisms. Compressive tests, direct tension test and four point bending tests were selected to be able to characterize the tensile strength and correlate it to the compressive strength. A total number of specimens of 360 dog-bone specimens, 70 prisms, and 42 cylinders were sampled from 12 batches. Aging and storage conditions varied from one batch to another. All conditions and variations between batches are explained and discussed in the following sections.

2.1 Materials and Mix Proportions

The used UHPC in this study is a commercial carbon nanofiber enhanced UHPC (CeEntek). The superiority of this UHPC is in a black paste, a superplasticizer (cePAA-80SDR) that contains 0.5% readily dispersed CNF and other admixtures. The CNF is intended to enhance the behavior and the bond strength between the mixed particles and steel fibers. The UHPC main components are (1) preblended and prebagged 50 lbs. dry mix (ce200 SF-g); (2) prepacked CNF paste with admixtures; (3) portable water; (4) steel fibers; and (5) a calcium nitrate accelerator. The CeEntek ingredients are shown in Figure 2.1a

2.2 Mixing procedure

UHPC typically requires a high shear mixer, low water-to-cement ratio, and absence of coarse aggregates necessitates different mixing procedures to ensure that a proper mix is

achieved, and the early setting is avoided with less mixing time. Imer Mortman 360 high-shear mixer was used in compliance with the manufacturer's recommendations. Mainly nine steps are performed; starting with (1) the molds where the UHPC will be cast are prepared and cleaned (2) applying a release agent to the molds (3) introducing the dry mix (ce200SF-G); (4) followed by the superplasticizer diluted cePAA-80SDR (Figure 2.1b) with potable water forming carbon nanofiber suspension; (5) an accelerator (Nitcal-Calcium Nitrate 70%) is added, and mixing continues for 7-9 minutes till the UHPC paste is formed (Figure 2.1c); (6) last step was adding the steel fibers; (7) wait to have a well-distributed fibers in the paste; (8) cast the UHPC into the molds; (9) transfer specimens to storage/curing (Figure 2.1d).

The UHPC was cast into three types of specimens: prisms, dog-bone, and cylinders. For both prisms and dog-bone specimens, the UHPC was poured into the form at one end and flowed toward the other end. Prismatic specimens were tested for flexural tests with dimensions of 3 by 3 by 12 inches (76.2 by 76.2 by 304.8 mm). Dog-bone specimens were tested for direct tension test with thicknesses of ½ inch (12.7 mm) and 1 inch (25.4 mm) (Figure 2.2) due to geometric limitations of the gripping mechanism of the testing machine. Cylindrical specimens were cast for assessing the compressive strength and relating it later to captured tensile behavior. The specimens were poured vertically into plastic cylinders with dimensions of 3 by 6 inches (76.2 by 152.4 mm). The exact number of specimens will be later explained in the Sampling section.

All specimens were cast at the construction yard outside the Earthquake Engineering Laboratory (EEL) at the University of Nevada, Reno and then transported either inside the

testing floor of EEL or to the basement of EEL. The temperature and humidity were mostly

constant for all batches and specimens: 21˚C (70 ˚F) and 50 percent of relative humidity.
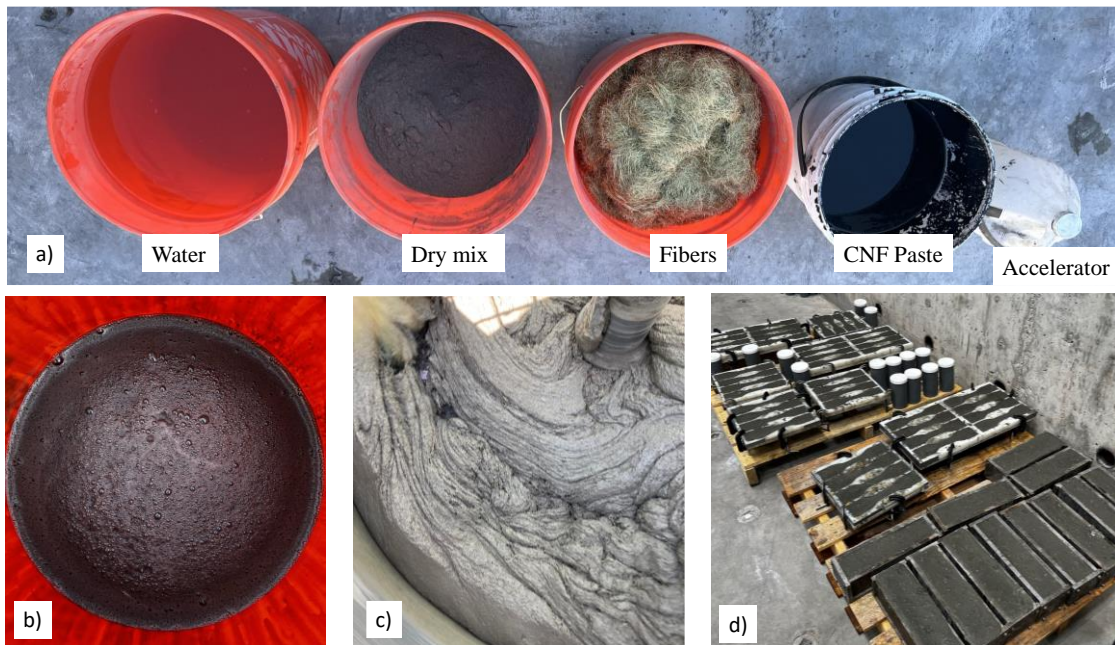
Figure 2-1 (a) UHPC components; (b) CNF paste after dilution with water forming CNF

suspension; (c) UHPC paste achieved; (d) Specimens are stored inside of Earthquake

Engineering laboratory at the University of Nevada, Reno
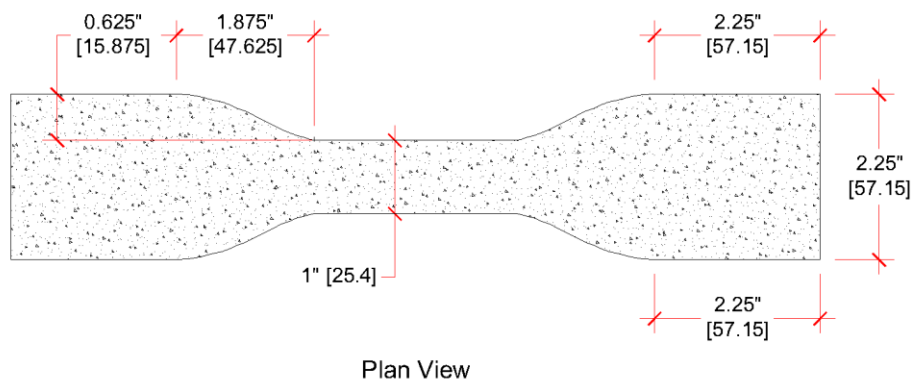
Figure 2-2 The dog-bone specimen's dimensions

A series of trials and batches were examined. A total of three proportions were carried out (Table 2.1). The first ratios were proposed by the manufacture and considered as a default mix. The second was an approach the research term took; trying to reach to an appropriate mix. The last mix was the manufacture's recommendation after reporting the testing results and quality issues of the mix. The second mix had 3% more additional water to mix. The third mix had half the amount of accelerator, 5% more water with 50% of the removed quantity of the accelerator will be added as water. The main issues that led to change of the proportions were flowability and early setting. Not only these reasons, but chunks of fibers and unmixed clumps were observed in the first 2 batches.

Table 2-1 The proportions for the three batches with varying steel fiber percentages.

Batches	SF [%]	Mix ingredients by weight lb./ft³				
		Steel fibers	Premix	Water	CNF paste	Accelerator
BA-1	0	0	146.5	10.3	0.84	1.46
	1	4.91	145	10.2	0.83	1.45
	2	9.76	143.6	10.1	0.83	1.44
	3	14.62	142.1	9.9	0.82	1.42
	4	19.47	140.64	9.78	0.82	1.41
BA-2	0	0	146.5	10.61	0.84	1.46
	1	4.91	145	10.5	0.83	1.45
	2	9.76	143.6	10.4	0.83	1.44
	3	14.62	142.1	10.2	0.82	1.42
	4	19.47	140.64	10.1	0.82	1.41
BA-3	0	0	146.5	11.18	0.84	0.73
	1	N.A.				
	2	9.76	143.6	10.97	0.83	0.72
	3	N.A.				
	4	19.47	140.64	10.62	0.82	0.7

2.3 Sampling

Three tests were utilized to investigate tensile strength and correlated to compressive strength. Direct tension test was the primary selected test applied on dog-bone shaped specimen that varied from 0.5 inch and 1 inch thickness. Letter "A" was designated for the one-inch thick specimens and "B" was designated for the half-inch thick. The second test was four bending test. It is an indirect way to capture tensile behavior as flexural reactions are a combination of tension and compression forces. Last test was compressive test on cylinders to correlate tension results to compressive strength. In total, an estimated 556 specimen was prepared, casted and tested. Number of specimens varied for each batch and test (Table 2.2). For BA-3 for each fiber dosage (the optimum batch), 14 cylinders were tested for compression, 12 prisms were tested for 4-point bending and 24 one-inch dog-bone and 20 half-inch dog-bone were tested for direct tension.

After casting the specimens, if testing is scheduled for 3 day mark, then demolding the specimens will take place on the 2nd day, otherwise demolding would be on 4th day. Specimens are kept at the basement of Earthquake Engineering laboratory at the University of Nevada, Reno till the test day.

2.4 Testing

2.4.1   Direct Tensile Test

All dog-bone specimens were tested under direct tension test using Instron 5985 testing machine (Figure 2.3a). Instron is an electromechanical testing system that has a capacity of 250 kN (56250 lbs.). To test a specimen, few steps were followed to ensure a successful

documentation and results. First step was to label the specimen according to a nomenclature that was set to all testing for all batches. It specified the specimen's number in the batch and testing day, steel fibers content, specimen size (A for 1 inch and B for ½ inch) and concrete's age. For example, S1_CE1_A_7D means the first specimen from the 1% fiber content of dog-bone size A (1-inch thick) tested after 7 days.

Table 2-2 The type and number of specimens for each batch.

	Type of Specimens	Number of Specimens				
		SF 0%	SF 1%	SF 2%	SF 3%	SF 4%
Batch #1	Prisms	6	10	6	6	6
	Size B Dog-bone ½"	5	20	1	10	10
	Size A Dog-bone 1"	N. A				
	Cylinders	N. A.				
	Type of Specimens	Number of Specimens				
		0%	1%	2%	3%	4%
Batch #2	Prisms	N.A.				
	Size B Dog-bone ½"	6	20	20	16	N. A.
	Size A Dog-bone 1"	6	16	16	16	
	Cylinders	N. A.				
Batch #3	Type of Specimens	Number of Specimens				
		0%	1%	2%	3%	4%
	Prisms	12	N. A.	12	N. A.	12
	Size B Dog-bone ½"	7		202		20
	Size A Dog-bone 1"	14		24		24
	Cylinders	15		13		14

Then, specimens' dimensions are recorded. Afterwards, testing method is selected and revised. Dog-bone specimens had two different sizes, which required adjusting the grips on the machine. Extensometer is checked to be ready and working. In case of the laser extensometer, reflective tape is applied on the specimen to be able to record extension on the specimens. After checking, the test starts ensuring the smooth recording of extension and load applied on the specimen (Figure 2.3b). The testing method used for direct tensile testing was displacement controlled; for the initial/elastic phase 0.02 inch per minute was applied till the specimen reaches the maximum load then, 0.12 inch per minute till the specimen reaches its failure (Figure 2.3c). The gripping mechanism that was available with the Instron machine limited the thickness of the dog-bone specimens to ½ and 1-inch specimens.
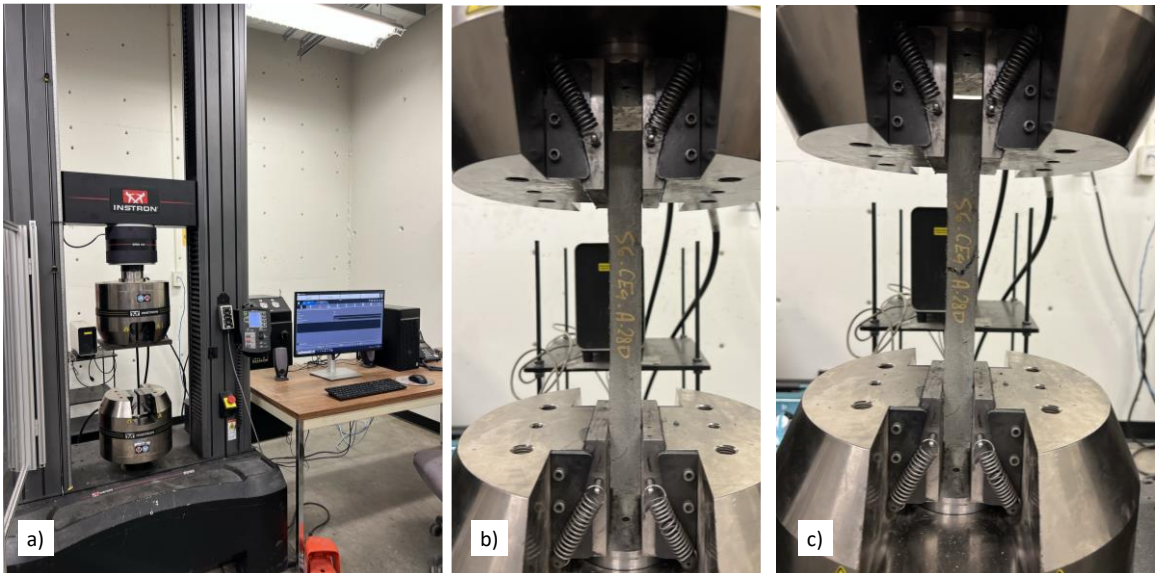
Figure 2-3 (a) Instron testing setup; (b) One-inch dog-bone specimen gripped and ready for testing; (c) Failure of the specimen

2.4.2   Four-Point Bending Test

Bending test was conducted using the same machine but with different setup (Figure 2.4a). All specimens were tested according to the ASTM 1609 specifications (ASTM 2019).

To test a specimen, similar steps to direct tension test were followed. (1) First step was to label the specimen according to a nomenclature that was set to all testing for all batches. It specified the specimen's number in the batch and testing day, percentage of steel fibers and concrete's age; S1_CE1_7D. (2) Then, specimens' dimensions are taken and recorded. (3) Afterwards, testing method is selected and revised. (4) two fixtures are placed on the lower and upper ends of the machine's head. (5) reflective tape is added to the specimens to be able to record deflection. (6) The specimen, lower and upper loading plates are added (Figure 2.4b). (7) Starting the test and ensuring the smooth recording of extension and load applied on the specimen. The testing method used for 4-point bending was based on displacement; for the initial/elastic phase 0.10 inch per minute was applied till the specimen reaches 40% of its peak load (Figure 2.4c). At the point, the machine stops, and the test is concluded.
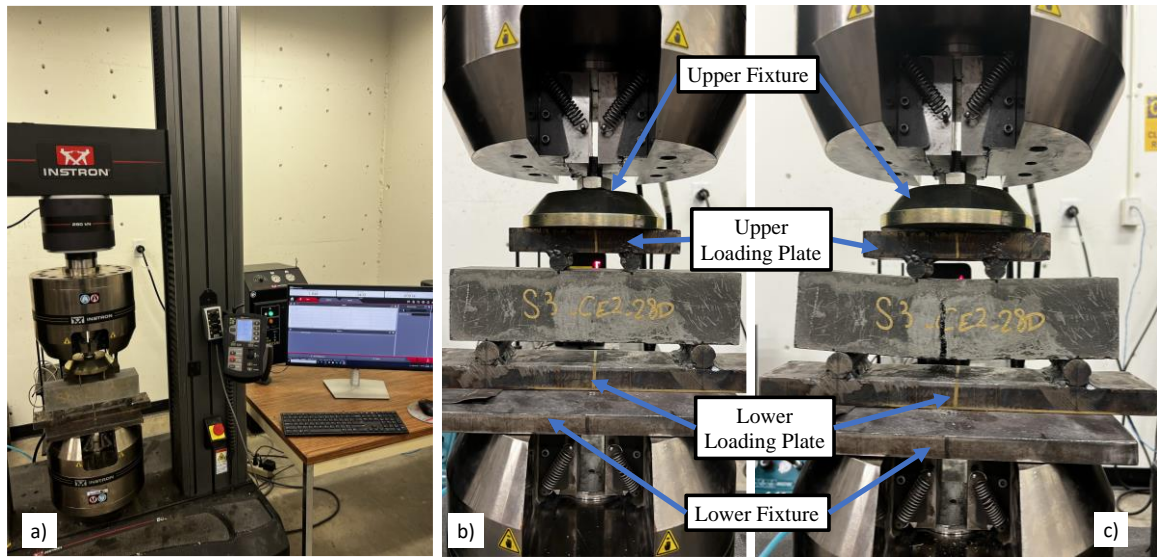
Figure 2-4 (a) Instron testing setup for 4-point bending; (b) A specimen is preloaded and ready for testing; (c) Failure of the specimen

2.4.3 Compression Test

Uniaxial compression test is one of the traditional concrete testing for compressive strength. In this study, it was utilized to corelate the tension behavior to compressive strength to. A SATEC machine with 500,000 lb. capacity was used on all cylinders to test their compressive strength (Figure 2.5a) Cylinders were 6 inches by 12 inches, a long process of preparation was followed to ensure having reliable results and to avoid any premature failure. Top surface of the specimens was cut off as they were not a good representative of their strength, then both ends were grinded to have smooth and parallel surfaces through the use of a fixed-end grinder (Figure 2.5b). After grinding, length to diameter ratios was not less than 1.83. The followed loading rate for the cylinders was 1000 lbs./sec. Breaking load was then recorded for further results analysis and interpretation (Figure 2.5c).
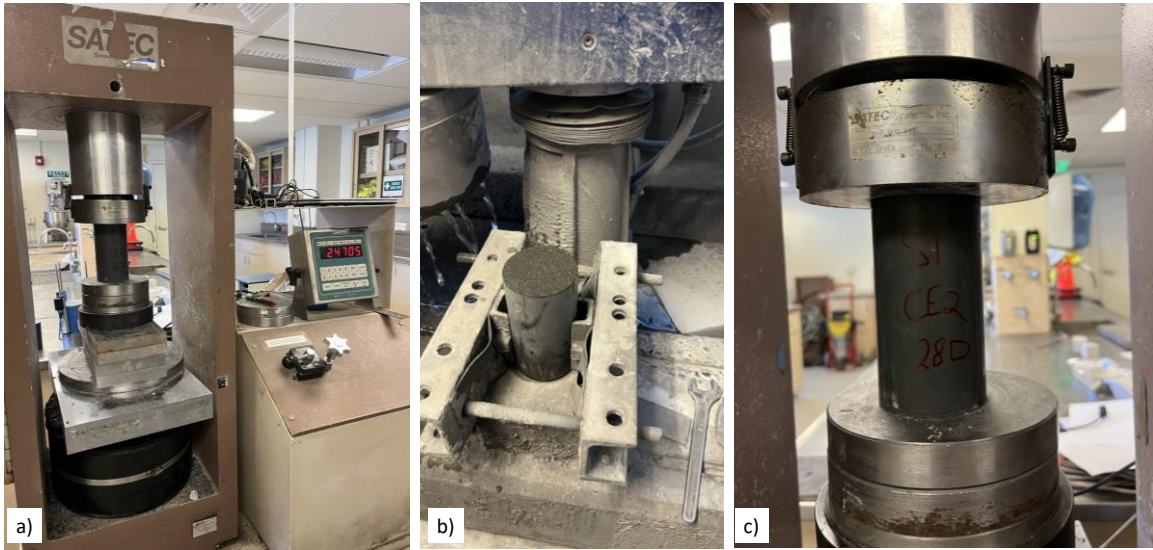
Figure 2-5 (a) SATEC machine setup for cylinders; (b) Preparation of a specimen for

testing; (c) Testing of the specimen

2.4.4   Testing Age.

Testing dates varied within the 3 batches. Testing mainly took place on 3, 7, 14, 21, and

28 days. Table 2.3 shows the number of specimens and testing age for the first batch. At

that point, research efforts have not explored the Size A one-inch dog-bone yet for more

reliable results. Also, cylinders were done by another member in the research team (Cimesa

& Moustafa, 2022).

For the second batch the Size A one-inch dog-bone was introduced and tested. Table 2.4

shows 2nd batch testing and number of specimens. Also, cylinders were casted and tested

by another member of the researcher team (Cimesa & Moustafa, 2022). The second batch

was the first trial to get more reliable results and had an increased percentage of water

content (3%) to help with flowability. No Prisms were casted at that time as the researcher

had acceptable results from previous batch but had inconsistent results from direct tension specimens.

Table 2-3 The number of specimens and testing age for the first batch

Type of Specimens	Number of Specimens (Testing age)				
	SF 0%	SF 1%	SF 2%	SF 3%	SF 4%
Prisms	3 (14D) 3 (28D)	2,3,2,3 (7D,14D,21D,28D)	3 (14D) 3 (28D)	3 (14D) 3 (28D)	3 (14D) 3 (28D)
Size B Dog-bone ½"	5 (28D)	5,5,5,5 (7D,14D,21D,28D)	1 (28D)	5 (14D) 5 (28D)	5 (14D) 5 (28D)
Size A Dog-bone 1"	N. A				
Cylinders	N. A.				

Table 2-4 The number of specimens and testing age for the second batch.

Type of Specimens	Number of Specimens				
	SF 0%	SF 1%	SF 2%	SF 3%	SF 4%
Prisms	N.A.				
Size B Dog-bone ½ "	3 (7D) 3 (28D)	4,4,4,4,4 (3D,7D,14D, 21D,28D)	4,4,4,4,4 (3D,7D,14D, 21D,28D)	4,4,4,4,4 (3D,7D,14D, 21D,28D)	4,4,4,4,4 (3D,7D,14D, 21D,28D)
Size A Dog-bone 1"	3 (7D) 3 (28D)	3,3,3,3,4 (3D, 7D ,14D, 21D,28D)	3,3,3,3,4 (3D, 7D ,14D, 21D,28D)	3,3,3,3,4 (3D,7D,14D, 21D,28D)	3,3,3,3,4 (3D,7D,14D, 21D,28D)
Cylinders	N.A.				

For the third batch, only specimens with steel fibers of 0%, 2% and 4% were casted and tested due the limited materials. All specimens were casted and tested and the third batch

had a different mix proportion than the previous batch as mentioned in section 2.2. Table

2.5 shows the number of specimens and testing age for the third batch.

Table 2-5 The number of specimens and testing age for the third batch.

Type of Specimens	Number of Specimens				
	SF 0%	SF 1%	SF 2%	SF 3%	SF 4%
Prisms	4,4,4,4 (7D,14D,28D)		4,4,4,4 (7D,14D,28D)		4,4,4,4 (7D,14D,28D)
Size B Dog-bone ½ "	0	N.A.	6,6,8 (7D,14D,28D)	N.A.	6,6,8 (7D,14D,28D)
Size A Dog-bone 1"	7,7 (14D,28D)		6,6,12 (14D,28D)		6,6,12 (14D,28D)
Cylinders	3,3,4,5 (3D,7D,14D,28D)		3,3,3,4 (3D,7D,14D,28D)		3,3,4,4 (3D,7D,14D,28D)

3. RESULTS AND DISCUSSION

All specimens were tested within the tolerances specified by ASTM C39 8.3. Direct Tensile and flexural tests were carried out on Instron machine 5985 located in the basement of Earthquake Engineering Laboratory, University of Nevada, Reno. All results showed are discussed and elaborated. It should be noted that all averages and specimens' results were vetted and a criteria similar to ASTM C39 with a tolerance of 10%-30% acceptance rate. If a specimen is outside the mentioned range, the researcher excludes it.

3.1 Flexural Testing Results

For the flexural testing two groups of results are presented as the 1st batch and 3rd batch only had prism specimens while the 2nd batch had only dog-bone specimens as was shown in Table 2-2. All graphs present averages of various fiber content and various maturity. The graphs show flexural stress also known as modulus of rupture which is calculated based on the x-axis and deflection which was recorded by the laser extensometer connected to the Instron machine on the y-axis.

$$\sigma_{fl} = \frac{PL}{b.d^2}$$

Equation 3-1-1

where P is the load applied, L is the span length, b is breadth of the specimen and d is the height of specimen.

Although specimens are assessed based on their average and considered as a sufficient representation, the researcher had a concern on the post peak behavior. When specimens have different strength, computing their average and plotting it will cloud areas of interest

in stress-deflection relationship. Figure 3-1 shows flexural stress-deflection relationship of individual specimens with their respective representative average. It shows how the variability of specimens' strength and location of their post peak behavior influence the average relationship as it suppresses some cracking and strain hardening features.
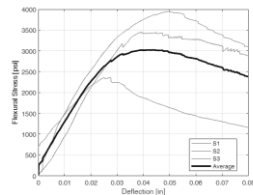
Figure 3-1 A specimen of an average flexural stress-deflection relationships with its individual specimens

First crack behavior was recorded for most specimens and a criteria was followed. In Figure 3.2 shows a stress deflection curve, where a sudden change in the relationship was noticed and it was characterized by a drop in the stress value followed by continuing climb or increase in the stress values. In general, 4% specimens across the board did not exhibit any similar behavior but had shown cracking during testing. Likely, that is attributed to the

dense amount of steel fiber having an adverse effect on closing the cracks and working along the material matrix.
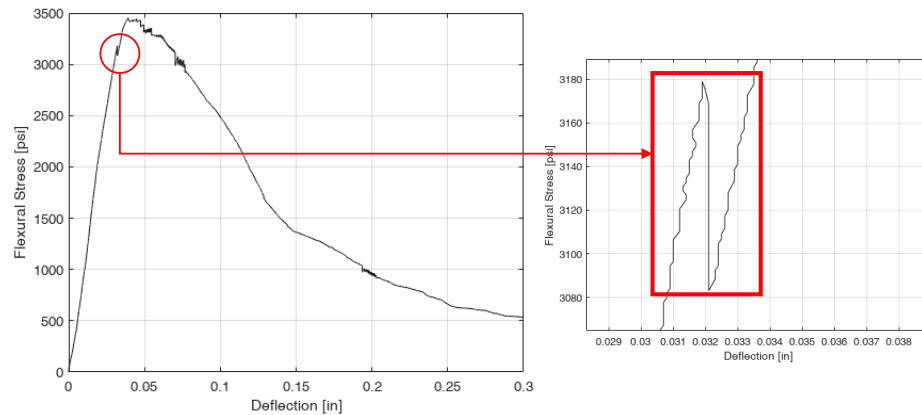
Figure 3-2 First crack criteria

Specimens' failures were similar in general context, very limited strain hardening followed by either rapid or slow decline in stress versus deflection. Strain hardening is a phenomenon where after the elastic phase and first cracking of the specimen a steady increase in capacity would be noticed preferably for a long deflection/strain value. In few specimens, it was noticed but for a very brief and short while. The first batch graphs specimens with no fibers showed brittle behavior. With adding fibers, overall behavior enhancement was noticed (Figure 3.3). In Figure 3.3 b, 14-day specimens show higher peak stress than the 28-day specimens. The researcher could not find an explanation for this behavior, but it might be variations in the specimens' curing, placing, or testing. On the other hand, it is likely to be attributed to insufficient curing as studies showed that UHPC may require additional curing regime than traditional concrete (Graybeal, 2006).

Specimens with 1-2-3% steel fibers content had moderate deterioration or reduction of capacity after maximum strength. Very subtle strain hardening was observed which was

followed by the deterioration. Contrary to previous behavior, 4% steel fibers specimens had a sudden loss of capacity once the specimens reached maximum strength. While the values of the maximum strength were clear in the 4% specimens, yet no favorable post peak behavior was recorded.

Increasing the fiber content from 0% to 1% resulted in an increase in strength by 82% and 12% in 14 and 28 days, respectively, while from 1% to 2% resulted in an increase in strength by 88% and 99% in 14 and 28 days, respectively. On the other hand, increasing fiber content from 2% to 3% resulted in an increase in strength by 3% and 15% in 14 and 28 days, respectively. Finally increasing the steel fiber content from 3% to 4% resulted in an increase in strength by 31% and 32% in 14 and 28 days, respectively.

The changes in deflections at peak stress were subtle and not significant. Differences were huge changing from 0% to 1% as it resulted in 1125% and 131% increase in 14 and 28 days, respectively. From 1% to 2%, there was a decrease by 23% and 13% in 14 and 28 days, respectively. From 2% to 3% an increase of 48% and 0.65% in 14 and 28 days, respectively. From 3% to 4% there was a decrease of 0.26% for 14 days but an increase of 13% for 28 days.

Deflection at first crack for prismatic specimens of the 1st batch was 1.35 ksi at 0.0125 in., 1.81 ksi at 0.0087 in., 1.97 ksi at 0.0094 in., 2.24 ksi at 0.0111 in. and 2.67 ksi at 0.0102 in. for 1%, 2%, 3% and 4%, respectively. Figure 3.3, Figure 3.4, Figure 3.5, and Figure 3.6 show flexural stress versus deflection relationship for 1st batch up to 0.08 and 0.15 inches of deflection on the x-axis as the first set of figures is zoomed in to demonstrate the initial behavior and strain hardening phases if any, while the second set shows the overall deflection till failure.

Figure 3-3 Close up view up to 0.08" deflection of average flexural stress-deflection relationships for the 1st batch prismatic specimens.

Figure 3-4 Average flexural stress-deflection relationships for the 1st batch prismatic specimens.

Figure 3-5 Close up view up to 0.08" deflection of average flexural stress-deflection

relationships for the 1st batch prismatic specimens.

Figure 3-6 Average flexural stress-deflection relationships for the 1st batch prismatic

specimens.

For the 3rd batch specimens, failure patterns were similar in the general context. Very

limited strain hardening followed by slow decrease in stress versus deflection. The third

batch graphs showed brittle behavior for specimens with no fibers. With adding fibers, the

overall behavior was enhanced as shown in Figure 3.6.

Increasing the fiber content from 0% to 2% resulted in an increase in strength by 262%, 354%, and 350% for 7, 14 and 28 days, respectively. While increasing from 2% to 4% resulted in an increase in strength by 169%, 126%, and 170% in 7, 14 and 28 days, respectively.

The changes in deflections peak stress were significant. The recorded changes from 0% to 2% were 892%, 913%, and 577% in 7, 14 and 28 days, respectively. Increasing from 2% to 4% resulted in increases of 72%, 111%, and 92% in 7, 14 and 28 days, respectively.

Deflection at first crack for prismatic specimens of the 3rd batch was 0.45 ksi at 0.0052 in., 2.77 ksi at 0.0276 in., and 7.31 ksi at 0.0717044 for 0%, 2%, and 4%, respectively.

Figure 3.6, Figure 3.7, Figure 3.8 and Figure 3.9 show flexural stress versus deflection relationship for the 3rd batch up to 0.08 and 0.15 inches of deflection on the x-axis as the first set of figures is zoomed in to demonstrate the initial behavior and strain hardening phases if any, while the second set shows the overall deflection till failure.
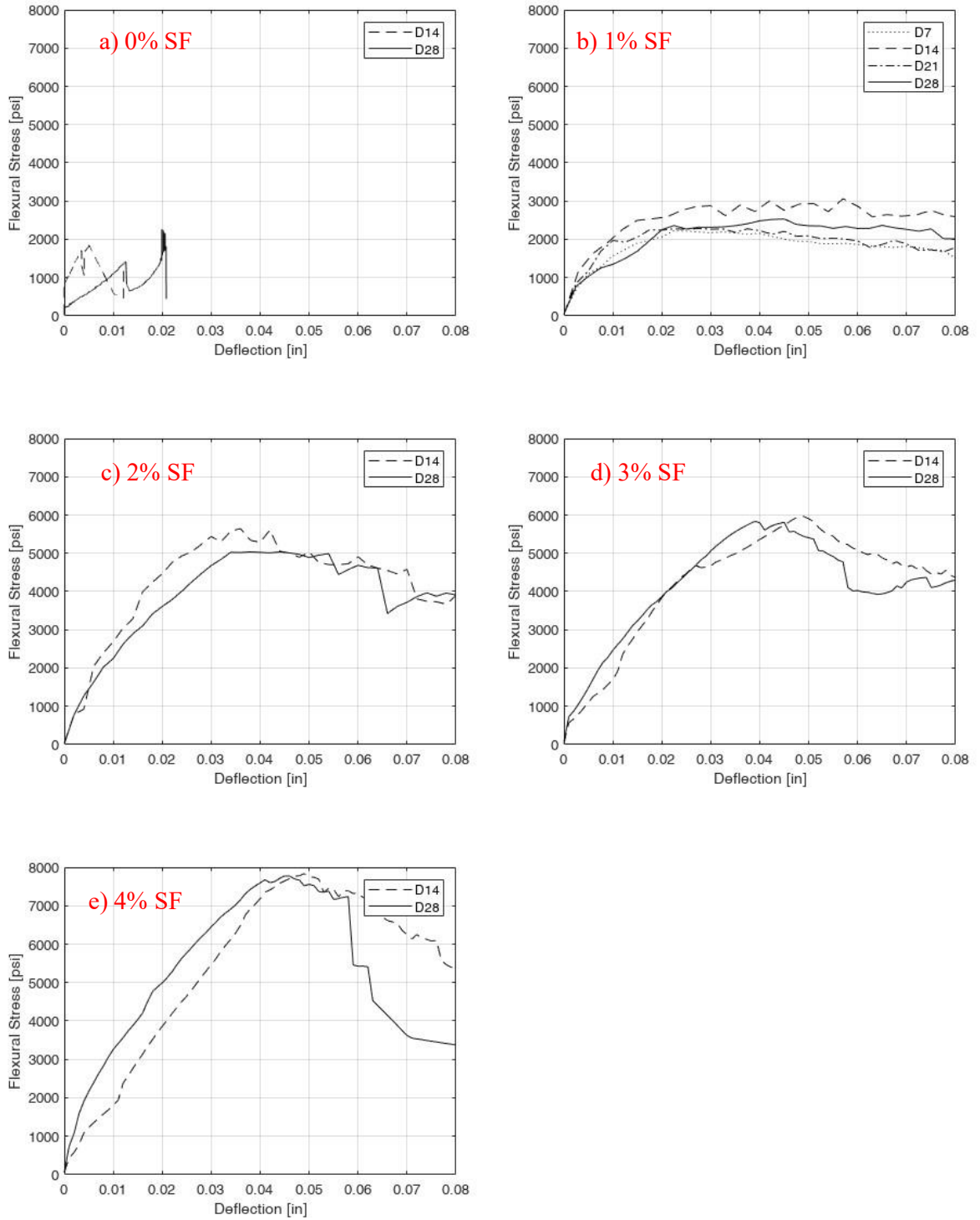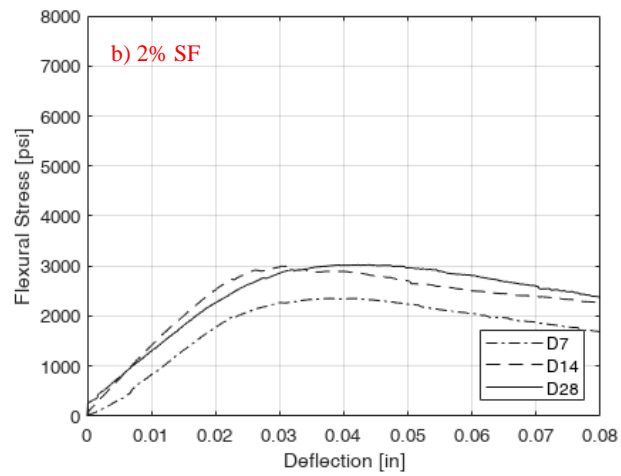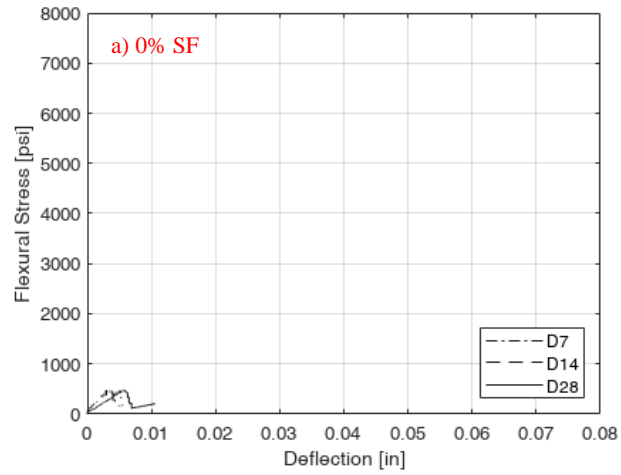
Figure 3-7 Close up view up to 0.08" deflection of average flexural stress-deflection

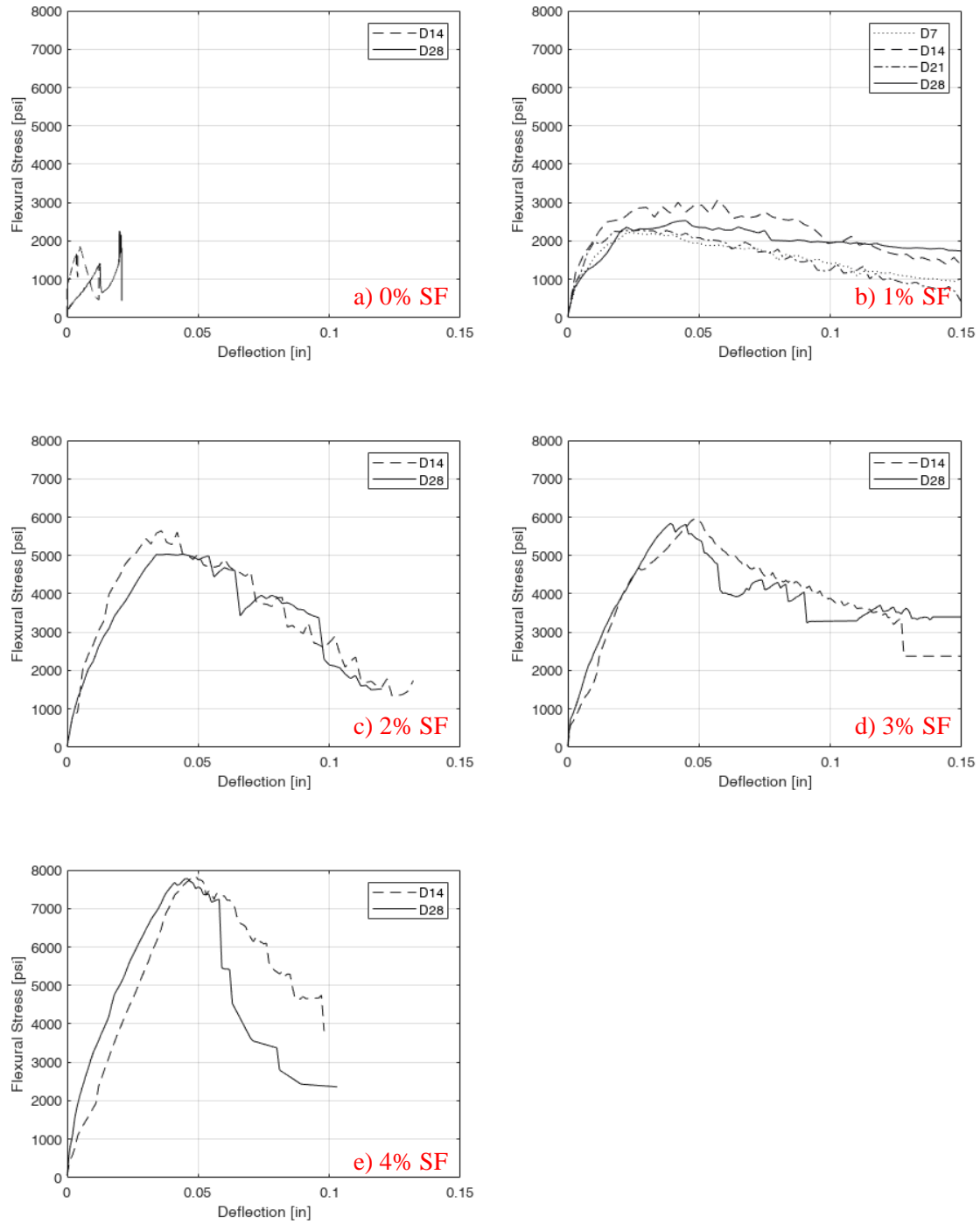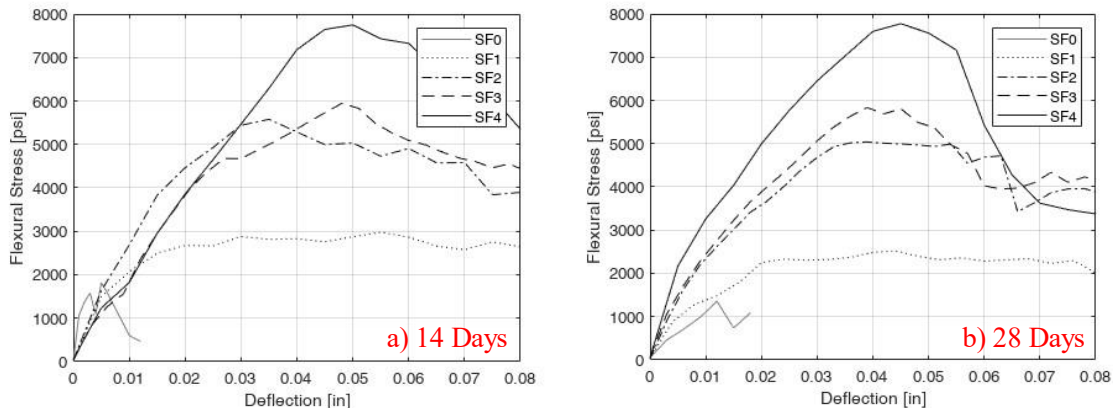relationships for the 3ʳᵈ batch prismatic specimens.
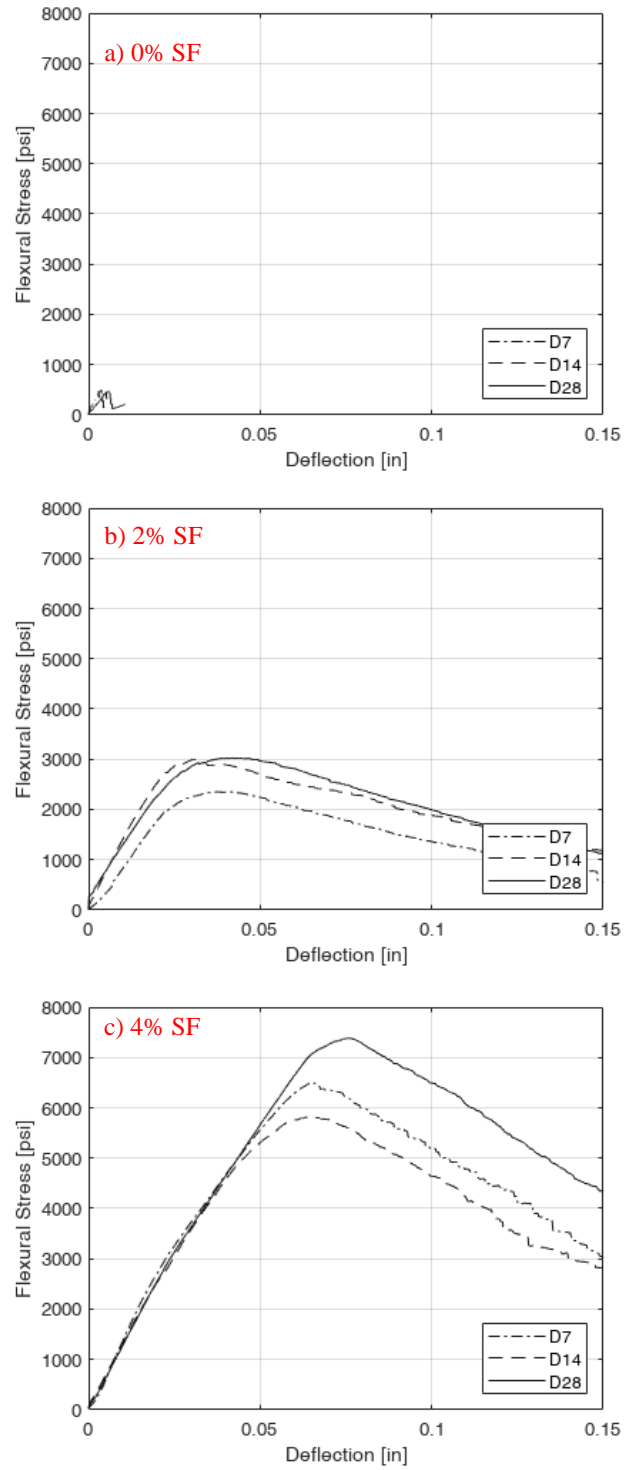
Figure 3-8 Average flexural stress-deflection relationships for the 3rd batch prismatic
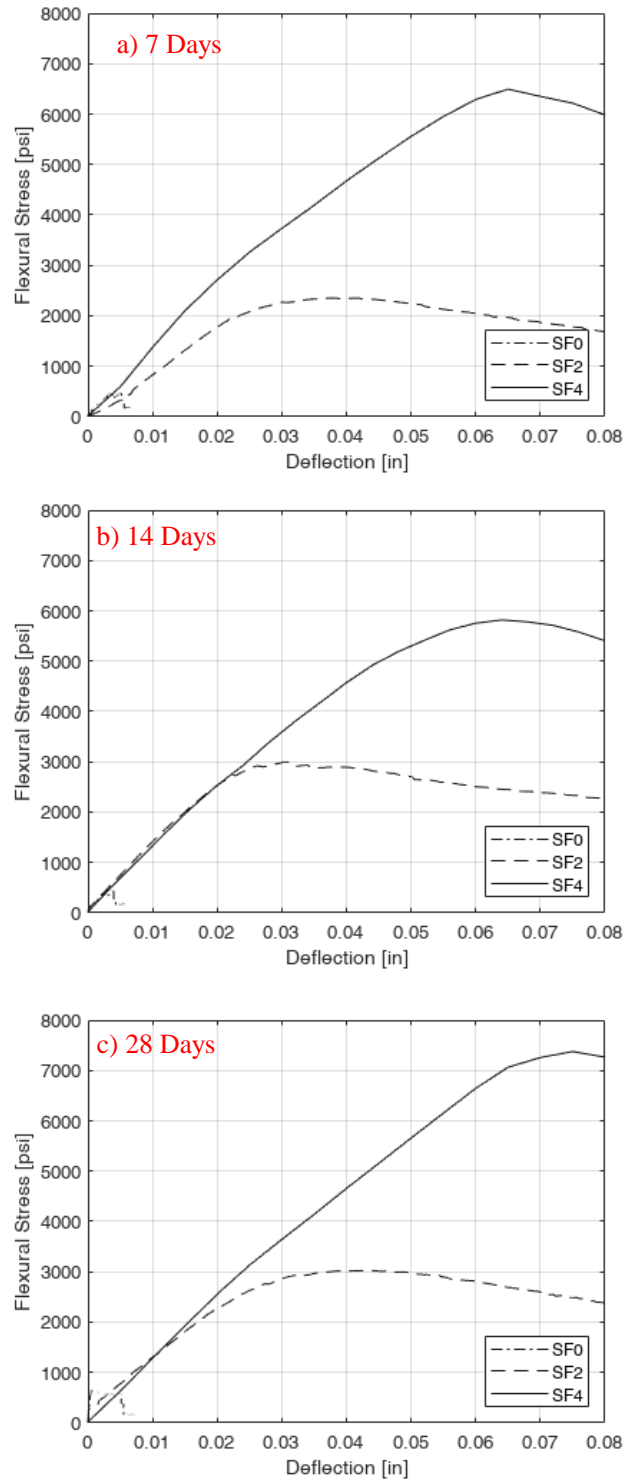
specimens

Figure 3-9 Close up view up to 0.08" deflection of average flexural stress-deflection
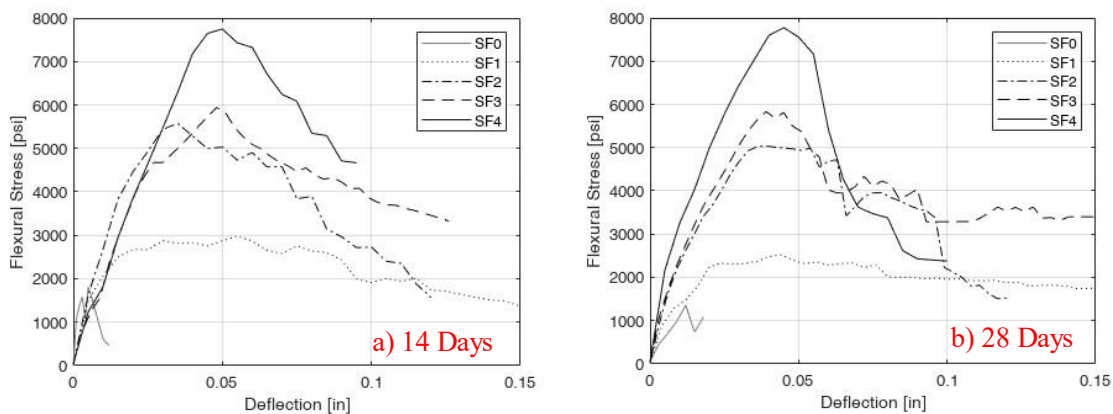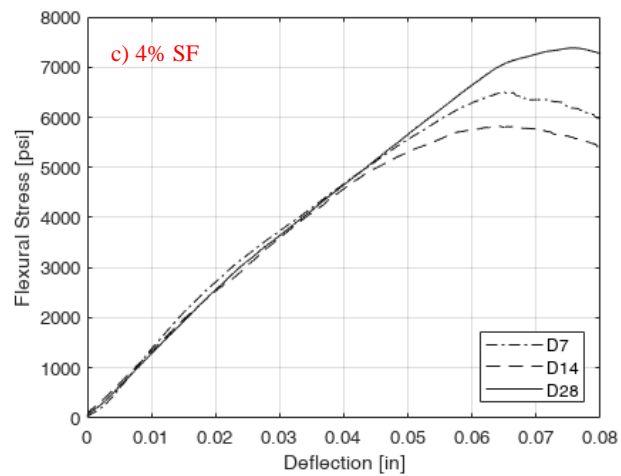
relationships for the 3rd batch prismatic specimens.
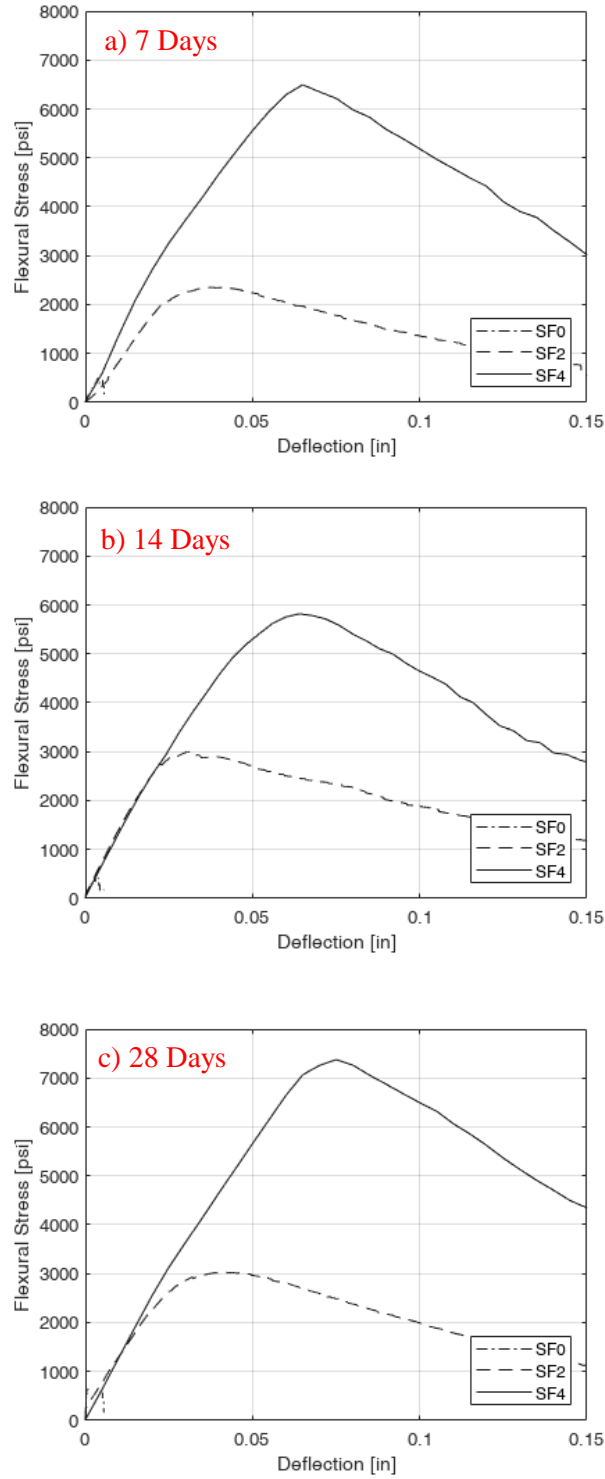
Figure 3-10 Average flexural stress-deflection relationships for the 3rd batch prismatic
specimens.

3.2 Direct Tensile Testing Results

3.2.1   Elastic Modulus

Elastic modulus is calculated based on the tensile stress-strain relationship, the slope between two points is calculated: 10% and 30% of the specimens' average strength. Determining the specimens' elastic modulus helps in characterizing the initial behavior or the elastic phase. Elastic phase is the initial part of the relationship between stress and strain, and it is named fully linear elastic. Normally it is concluded by the first crack of the specimen. Figure 3-11 shows the elastic modulus of dog-bone specimens for Size A and Size B of the 3rd batch.
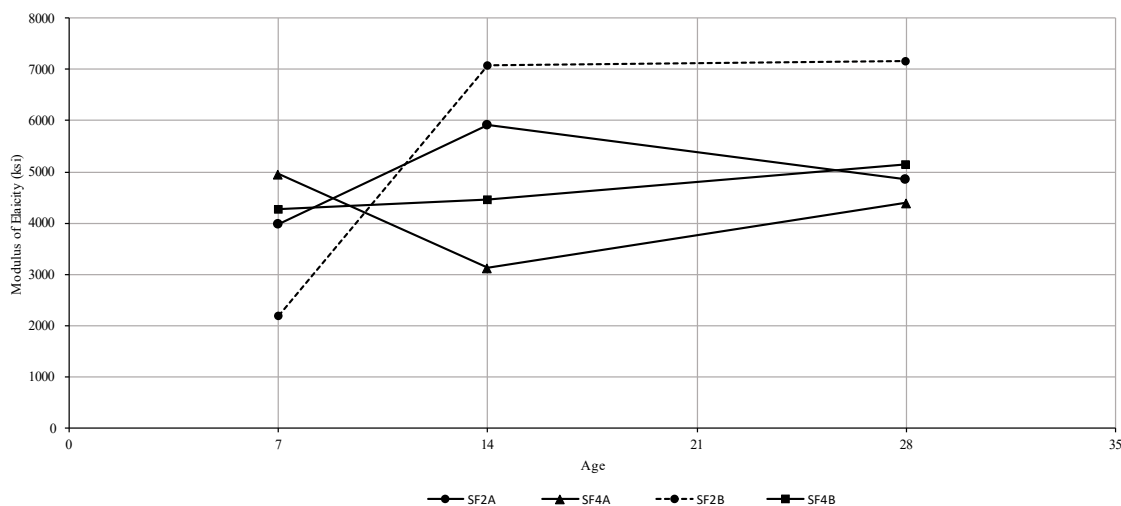
Figure 3-11 Modulus of elasticity of dog-bone specimens.

All three batches' results for the direct tensile testing are presented in the following section. Graphs present averages of various fiber percentages and various maturity. A total of 160 Size B ½ inch dog-bone specimens and 130 Size A1-inch dog-bone specimens were tested. The graphs show on the y-axis tensile stress and on the x-axis tensile strain. The strain was

recorded by the laser extensometer connected to the Instron machine. Tensile stress is simply calculated as tensile force generated by the Instron machine divided by the area

$$\sigma_{tensile} = \frac{P}{b.d}$$

Equation 3-2-1

where failure (crack) was located (Equation 3.2.1).

where P is the applied load, b is the breadth of the specimen and d is th e height of the specimen.

For the direct tensile test, the 3 batches had specimens of the ½ inch dog-bone while only the second and the third batches had specimens of the 1-inch dog-bone. The 3rd batch had only 0-2-4% specimens. For one-inch specimens with no fibers, specimens were successfully tested at 14 and 28 days. They were significantly harder to demold out of their cast despite using an industrial release agent. They were fragile and more prone to cracks and failure before testing. Some specimens had hairline cracks before demolding them. Drying shrinkage has made them very difficult to be extracted for testing. Curing might be a solution to this problem to further solidify the data and results, but it is not reliable as it is not applicable in field. In this respect the specimens with no steel fiber were once air cured in the Earthquake Engineering Laboratory. An attempt was made where constant humidity was guaranteed. During curing, specimens were covered by a plastic sheeting to maintain humidity level (Figure 3-12).
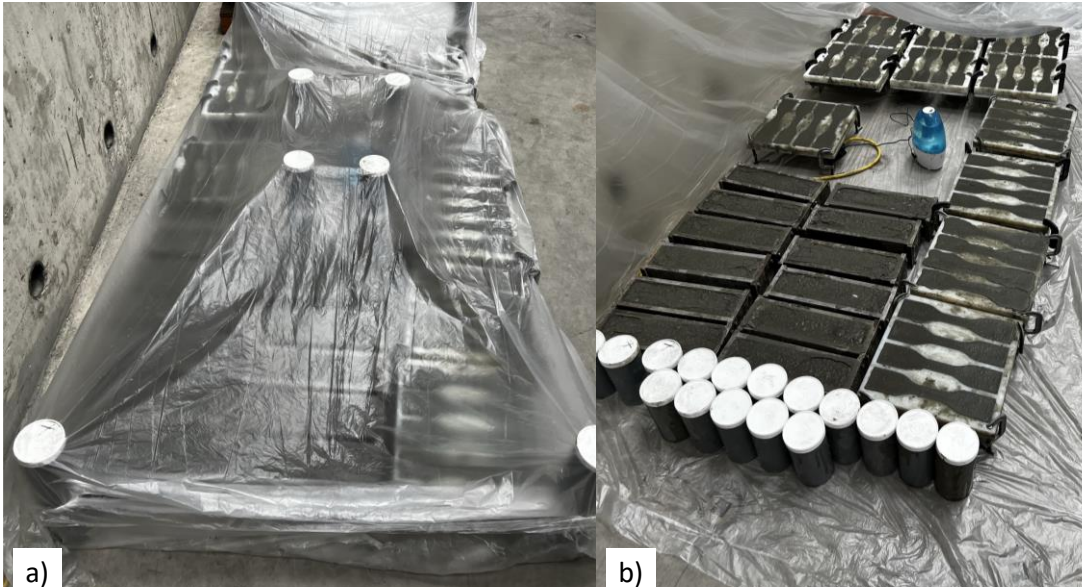
Figure 3-12 An example for curing of selected specimens with no fiber

Figure 3-13 to Figure 3-28 in the following subsections show tensile stress-strain relationships for all batches with both sizes dog-bone, sets of zoomed in graphs are included to highlight the initial phase of tensile behavior, followed by zoomed out graphs to provide full tensile stress-strain graphs. For Size B, ½ inch dog-bone, 0% specimens were all broken prior to testing, so no results were available to present. In general, Size B (0.5 inch) had significant higher values than Size A (1 inch) which show the unreliability of the results of Size B.

3.2.2   Half Inch Specimen: results grouped by steel fiber content

Limited development in strength was noticed in respect for maturity, with few specimens varying. Maturity did not attribute much to strength as the tensile strength purely depends on the fibers pulling out and bridging cracks and not the ageing of the material. Younger

age specimens on occasion show higher values of tensile strength than older ones. The reasonable explanation was variance in placing or curing of the specimens.

First and second batch results were grouped together for simplicity to show specimens with 1-2-3% steel fiber content results. Significant variance can be noted in the results. This was attributed to poor quality of the mix and placing creating voids, balls of dry powder or even clumps of fibers in the mix.

Half inch dog-bone size B most numbers were not justified as it was significantly higher than one inch Size A. For half inch dog-bone Size B 28-day results, increasing the fiber content from 1% to 2% resulted in a decrease of strength by 4%, while from 2% to 3% resulted in an increase in strength by 8% and from 3% to 4% resulted in an increase in peak strength by 9%.On the other hand for 14-day results, increasing the fiber content from 1% to 2% resulted in an increase in strength by 16%, while from 2% to 3% resulted in a decline in strength by 21%. Finally, from 3% to 4% resulted in an increase in peak strength by 169%. While for the 3rd batch increasing the fiber percentage from 2% to 4% resulted in a decrease in strength by 9% for 28 days.

Increasing fiber content from 1% to 2% resulted in a decrease in strain at peak strength by 35% and 14% decrease in 14 and 28 days, respectively. While from 2% to 3% it declines by 24.72% and increases by 56.62% in 14 and 28 days and from 3% to 4% there was a decline by 24.74% and 20.96% in 14 and 28 days, respectively. While for 3rd batch specimens resulted in an increase by 18% when increasing from 2% to 4% for 28 days results.

Figure 3-13 Close up view up to 0.005 strain of average tensile stress-strain relationships

for 1st and 2nd batch ½ inch dog-bone.

Figure 3-14 Average tensile stress-strain relationships for 1st and 2nd batch ½ inch dog-

bone.

Figure 3-15 Close up view up to 0.005 strain of average tensile stress-strain relationships

for 3rd batch ½ inch dog-bone.

Figure 3-16 Average tensile stress-strain relationships for 3rd batch ½ inch dog-bone.

3.2.3 Half Inch Specimens: results grouped by age

Stress at first crack was monitored by examining the stress-strain curves. After stress at first crack was recorded, an average of these values was computed and is considered as a representative value for the whole batch of specimens. It is worth mentioning that not all specimens had similar behavior present in their tensile stress-strain graphs while exhibiting cracks during testing. Specimens with 4% fiber content were the least to demonstrate any cracking during loading. This is attributed to the dense amount of steel fiber having a positive effect on distributing very fine undetectable cracks.

For ½ inch dog-bone specimens of the 1st and 2nd batch stress and strain at first crack was 0.73 ksi at 0.000664 strain, 1.034 ksi at 0.00055 strain, 0.89 ksi at 0.000337 strain and 1.24 ksi at 0.00123 strain for 1%, 2%, 3% and 4%, respectively while for the 3rd batch it was 1.33 ksi at 0.00018 strain and 2.245 ksi at 0.0011 strain for 2% and 4% respectively.

Figure 3-17 Close up view up to 0.005 strain of average tensile stress-strain relationships

for 1st and 2nd batch ½ inch dog-bone.

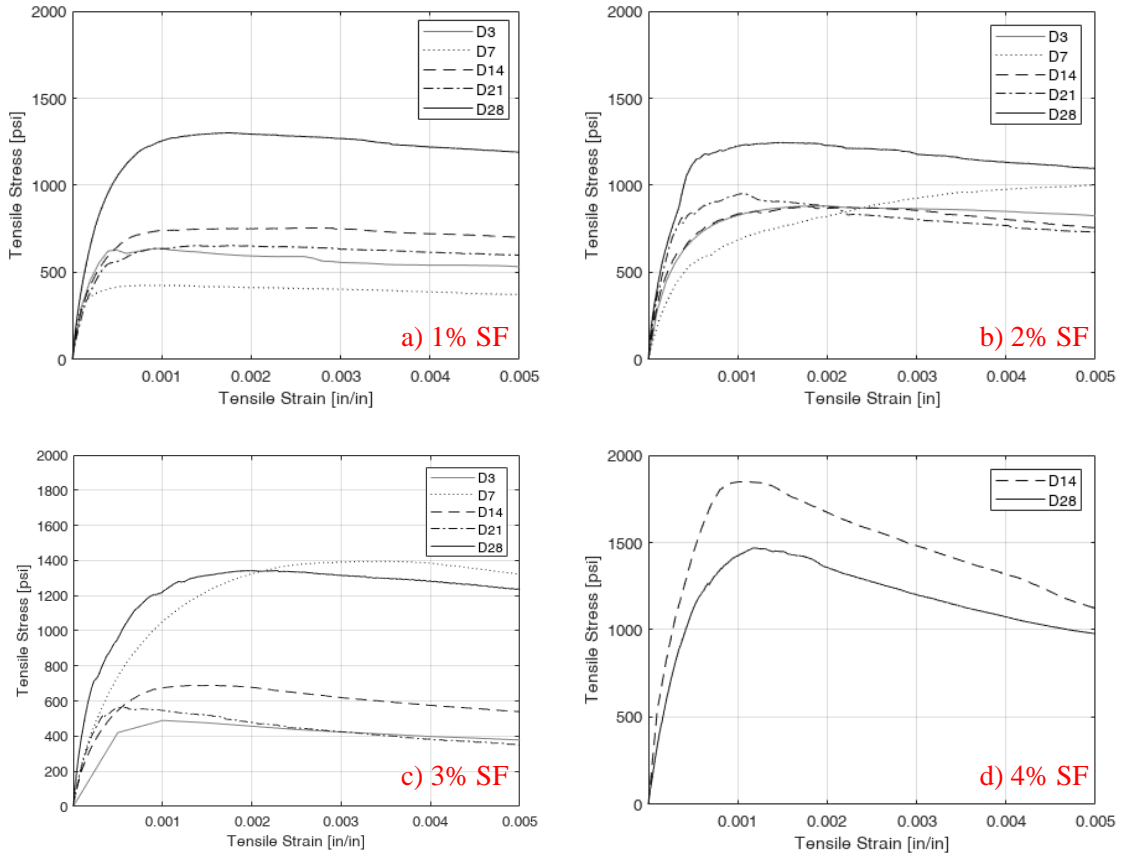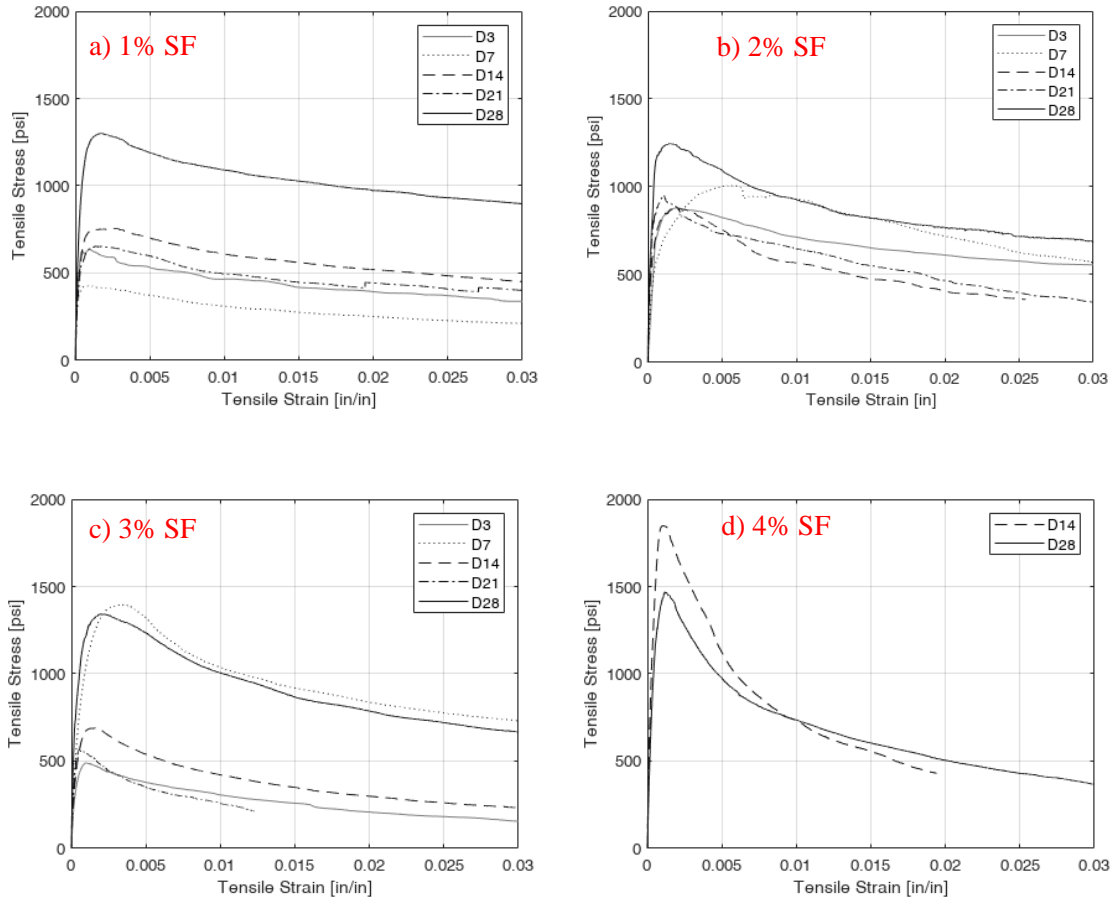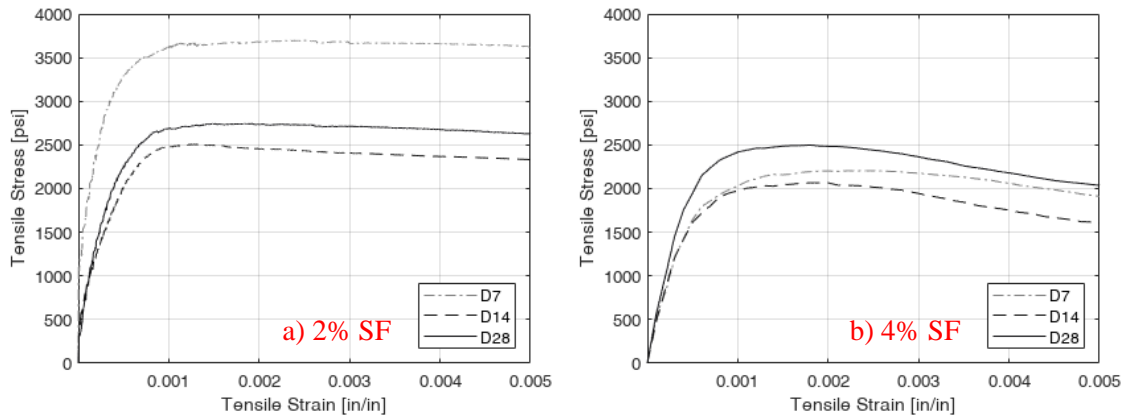Figure 3-18 Average tensile stress-strain relationships for 1st and 2nd batch ½ inch dog-

Figure 3-19 Close up view up to 0.005 strain of average tensile stress-strain relationships
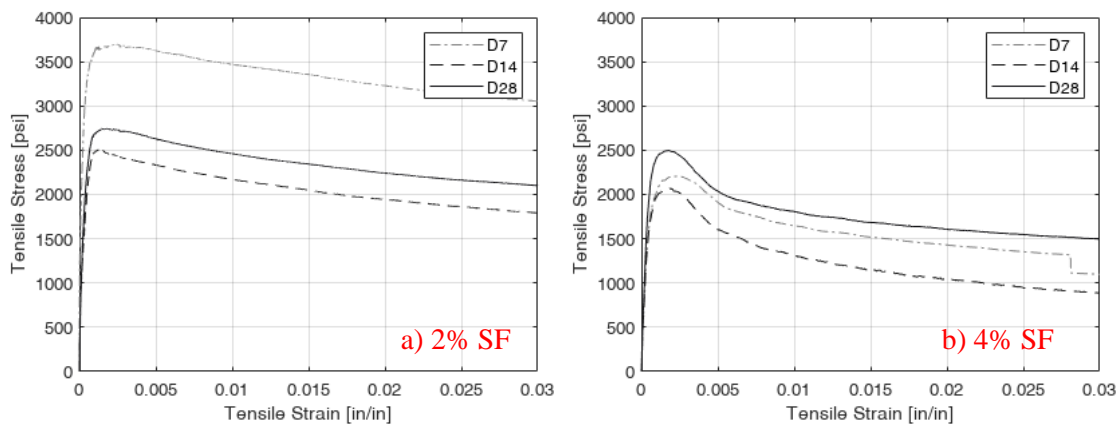
for 3rd batch ½ inch dog-bone.

Figure 3-20 Average tensile stress-strain relationships for 3rd batch ½ inch dog-bone.

3.2.4   One Inch Specimen: results grouped by steel fiber content

For 1 inch dog-bone Size A specimens 28-day results, increasing the fiber content from 1% to 2% resulted in a decrease in peak strength by 25%, while from 2% to 3% resulted in an increase in peak strength by 16% while for 14-day results, increasing the fiber content from 1% to 2% resulted in an increase in strength by 64%, while from 2% to 3% resulted in an increase in strength by 25%. For the 3rd batch, increasing the fiber percentage for 28 days from 0% to 2% resulted in an increase in peak strength by 252%, while from 2% to 4% resulted in an increase of strength by 8%.

The changes in strains at peak strength were subtle and slight. Differences was noted in 1 inch dog-bone Size A as from 1% to 2% it resulted in a decrease by 43% and 17% in 14 and 28 days, respectively. On the other hand, increasing the fiber content from 2% to 3% led to an increase in strain by 60% and 334% in 14 and 28 days, respectively. For 3rd batch specimens strain values, for 28 days results increasing fiber percentage from 0% to 2%, resulted an increase in peak strain values by 210% while from 2% to 4%, resulted a decrease in peak strain values by 3%.

The strain at first crack for 1 inch dog-bone specimens of the 1st and 2nd batch was 0.70 ksi at 0.00028 strain, 0.67 ksi at 0.00029 strain and 0.55 ksi at 0.0094 strain for 1%, 2% and 3% respectively. The first crack strain recorded for the 3rd batch was 2.005 ksi at 0.00076 strain and 2.189 ksi at 0.0009 strain for 2% and 4% respectively. Figure 3-25 and Figure 3-26 have a note on 28 days results calling anomaly, it is not expected or normal for the 3% steel fiber content to have weaker tensile strength than 1% or 2%. All specimens tested

for 28 days had similar results, which can be attributed to curing or placing factor but not representative to 3% specimens
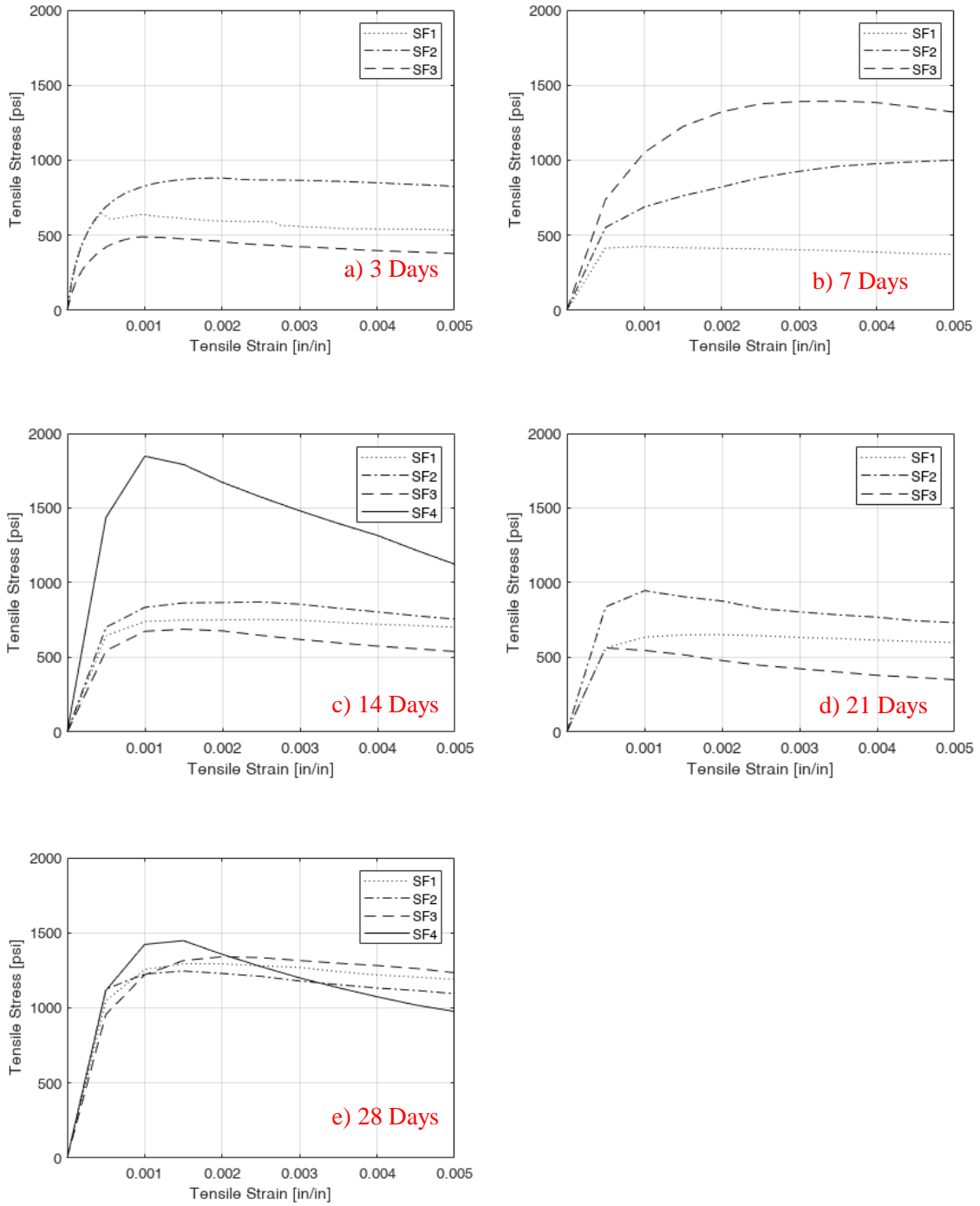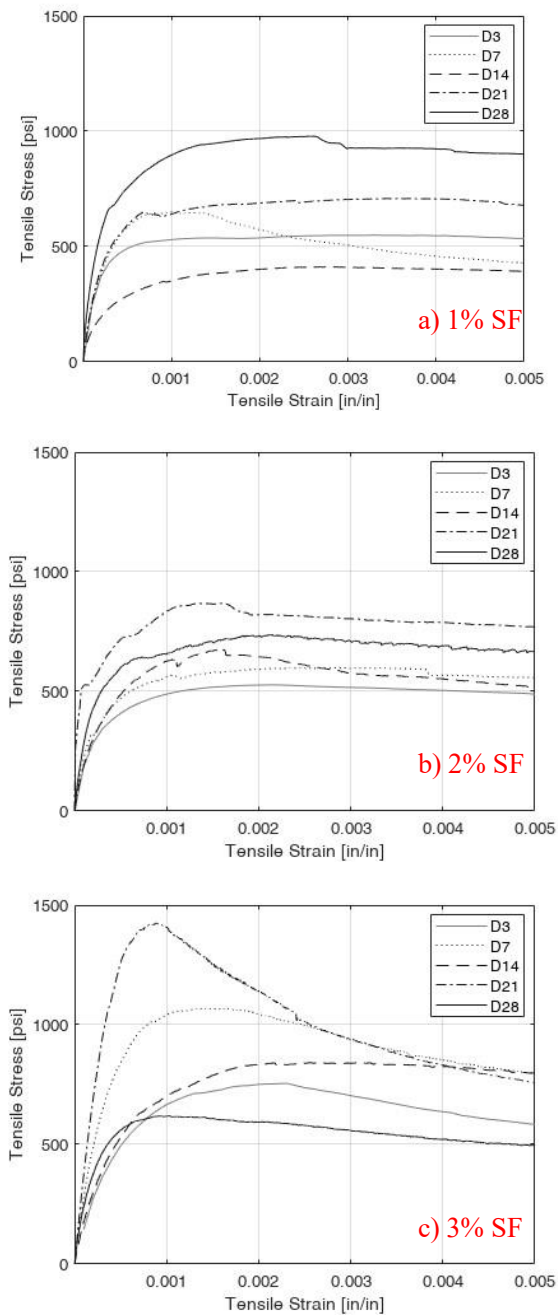

Figure 3-21 Close up view up to 0.005 strain of average tensile stress-strain relationships for 1st and 2nd batch 1 inch dog-bone.
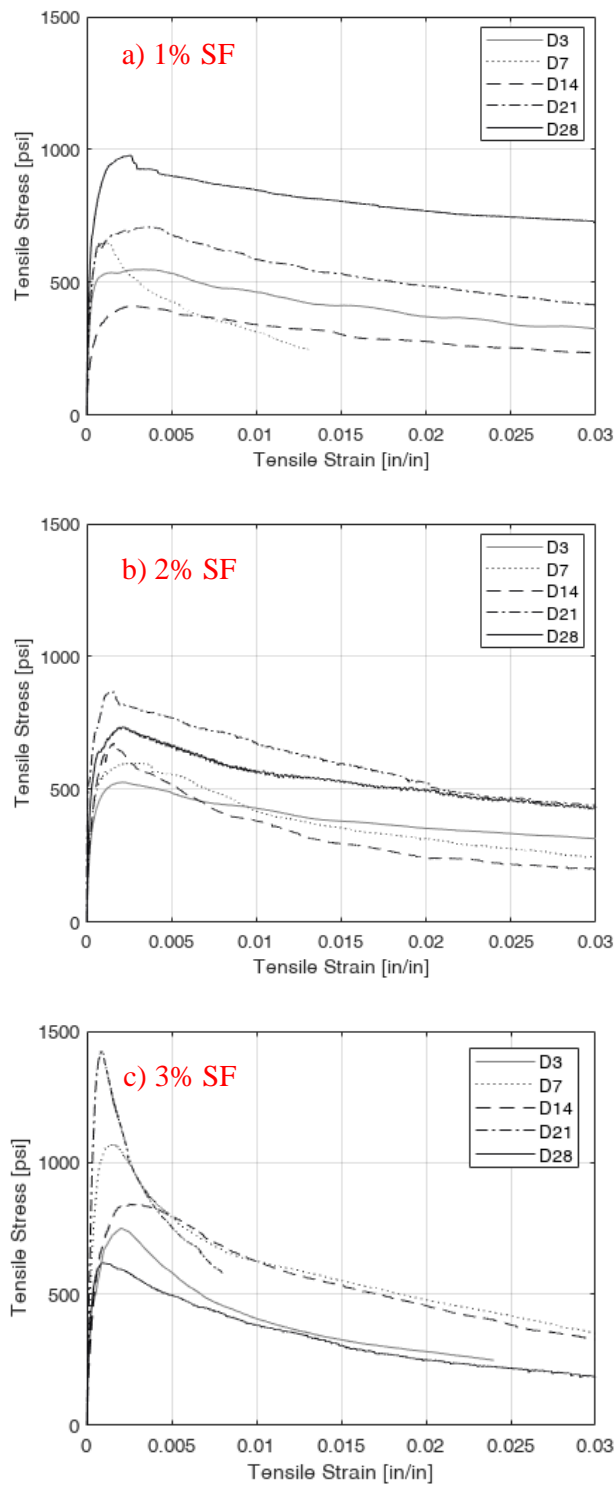
Figure 3-22 Average tensile stress-strain relationships for 1ˢᵗ and 2ⁿᵈ batch 1 inch dog-bone.
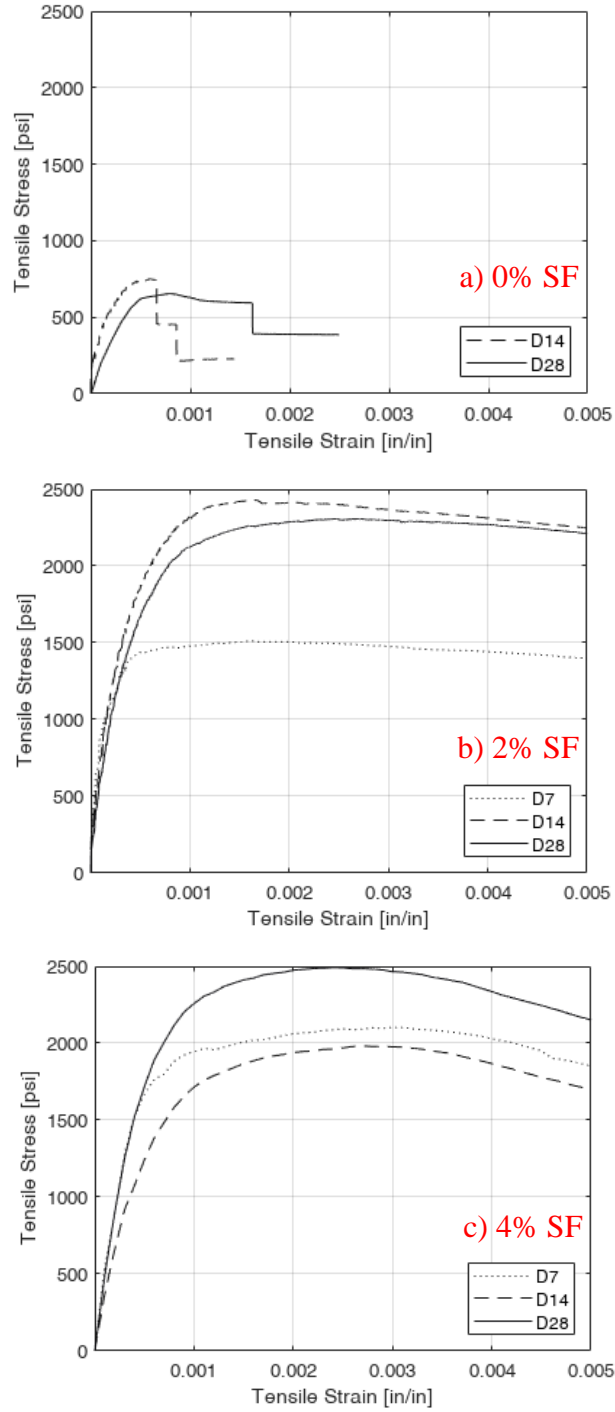
Figure 3-23 Close up view up to 0.005 strain of average tensile stress-strain relationships

for 3rd batch 1 inch dog-bone.
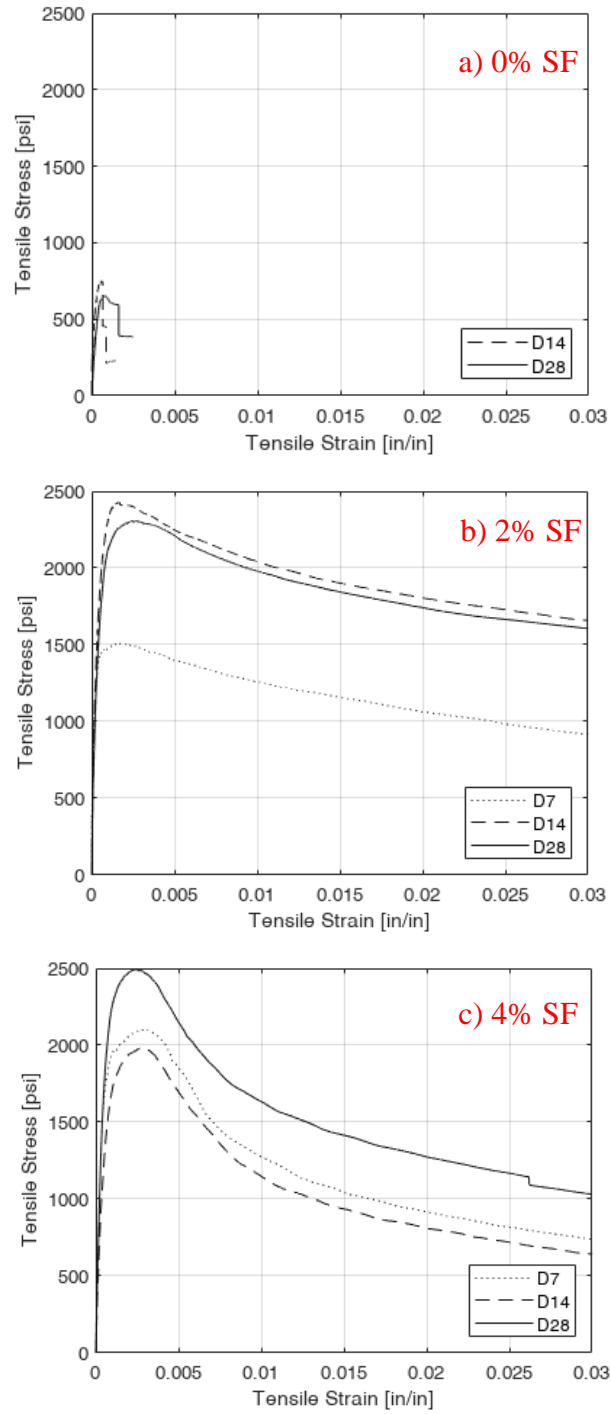
Figure 3-24 Average tensile stress-strain relationships for 3rd batch 1 inch dog-bone.

3.2.5   One Inch Specimens: results grouped by age
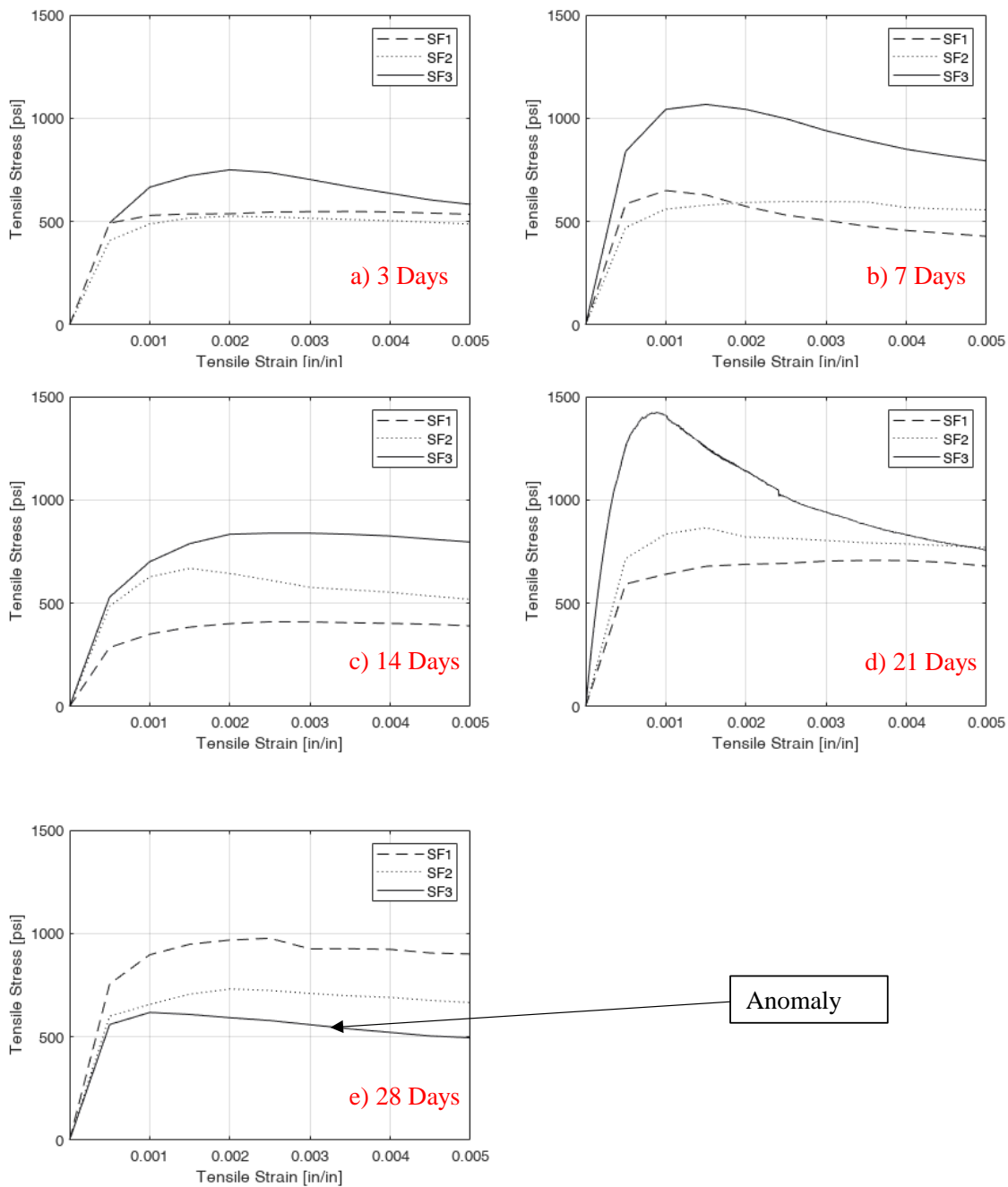
Figure 3-25 Close up view up to 0.005 strain of average tensile stress-strain relationships

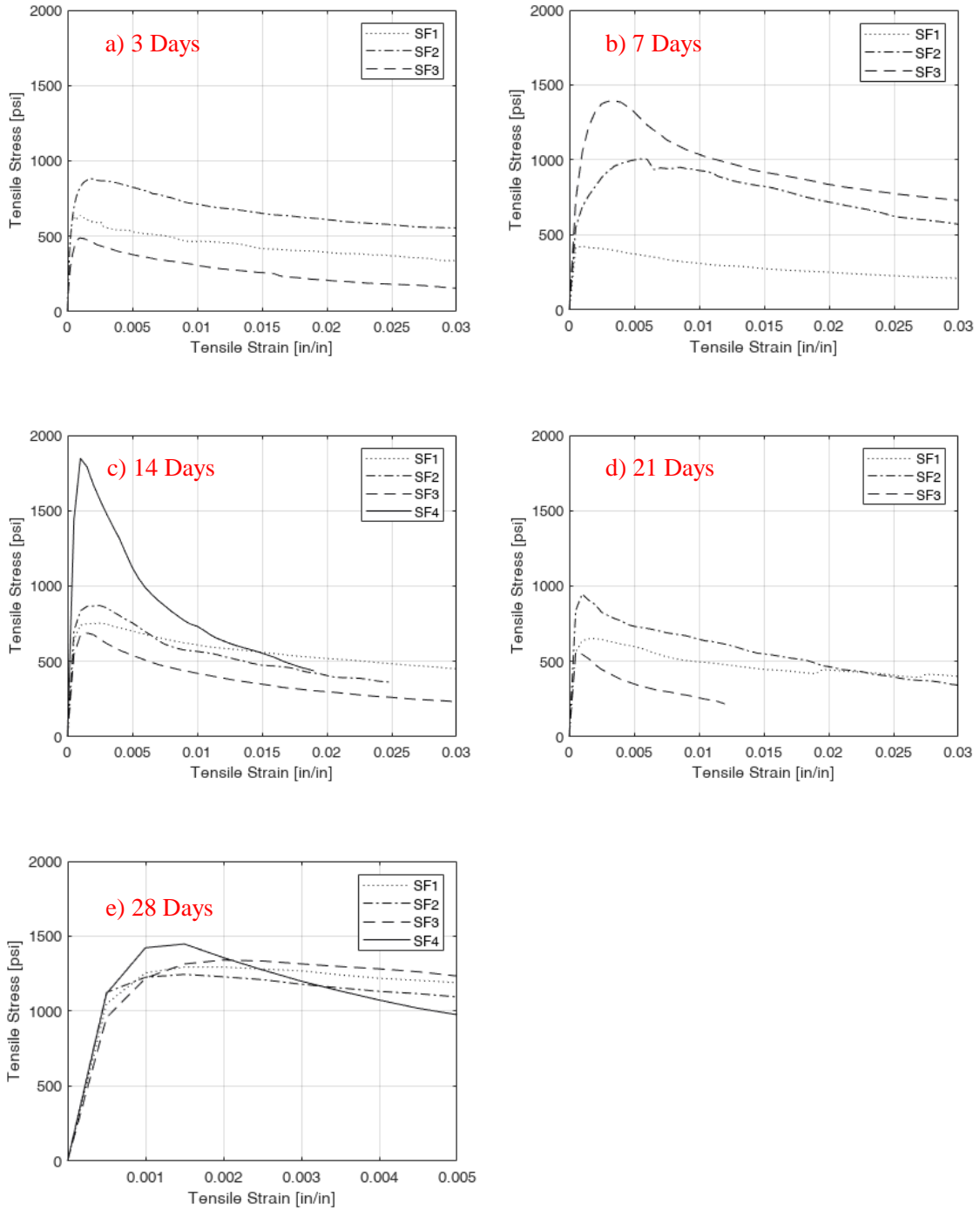for 1st and 2nd batch 1 inch dog-bone.
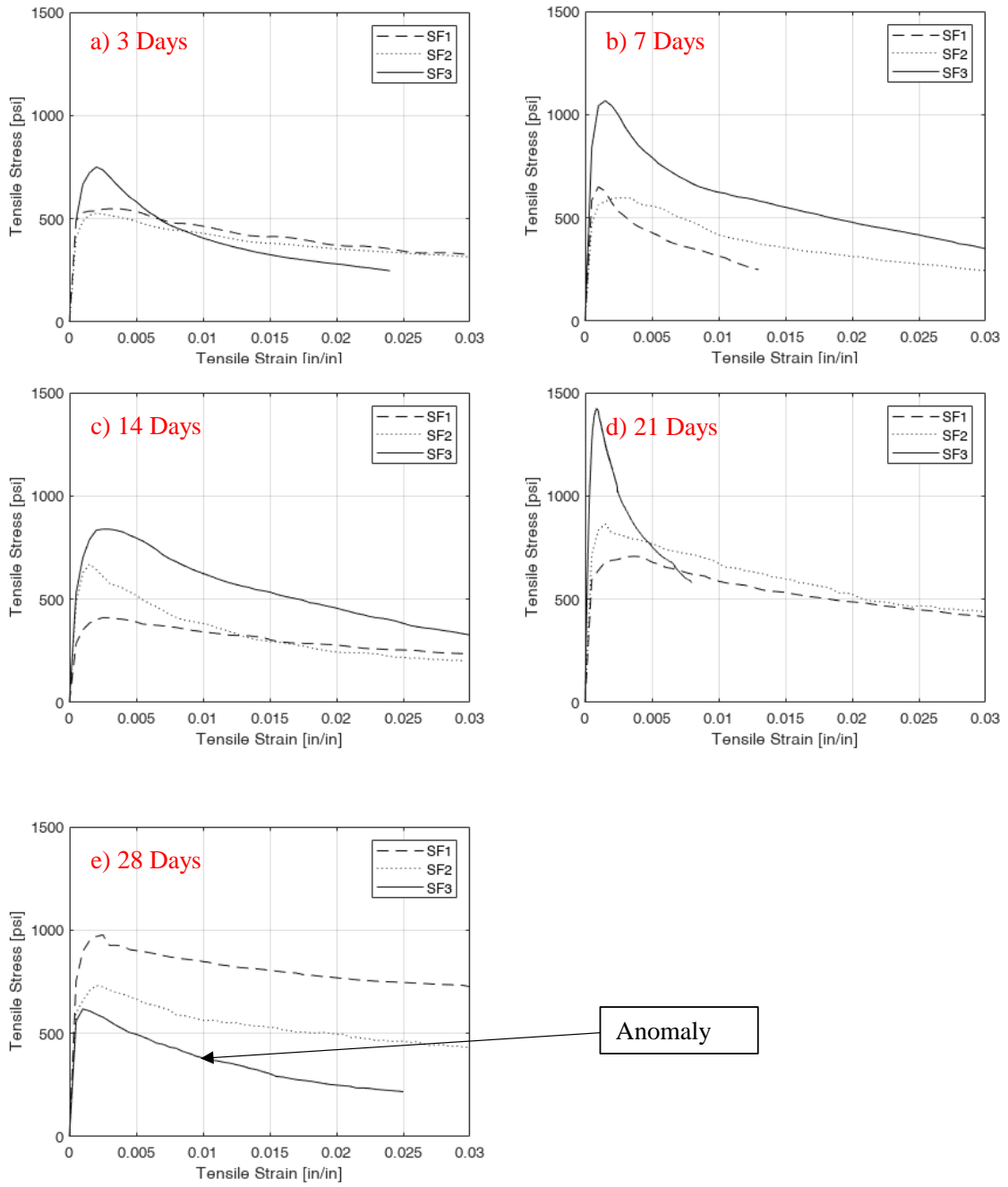
Figure 3-26 Average tensile stress-strain relationships for 1st and 2nd batch 1 inch dog-
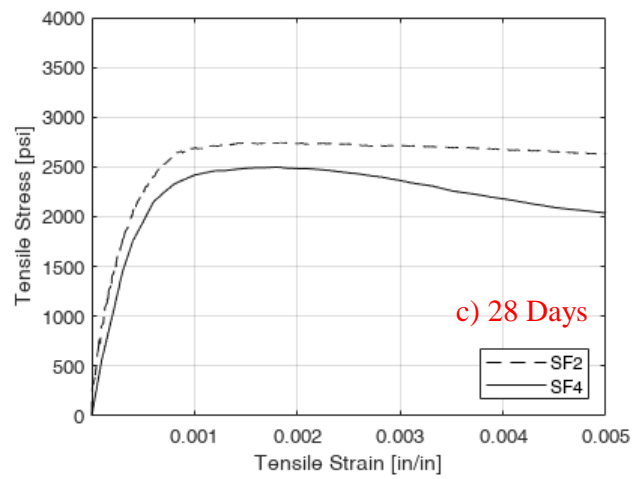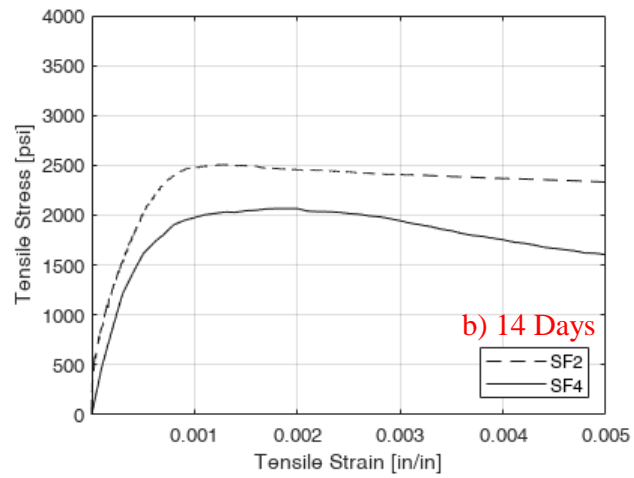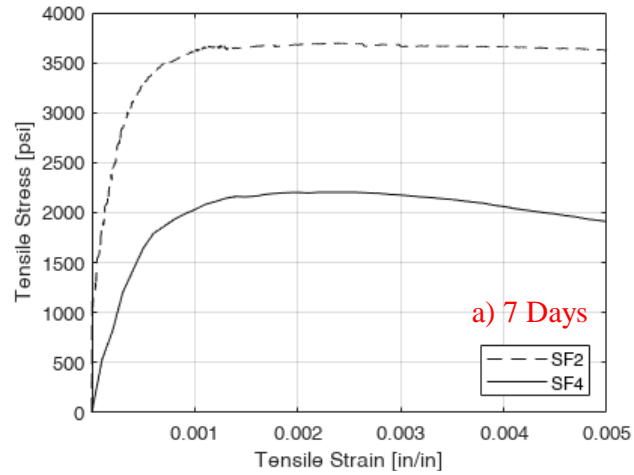
bone.
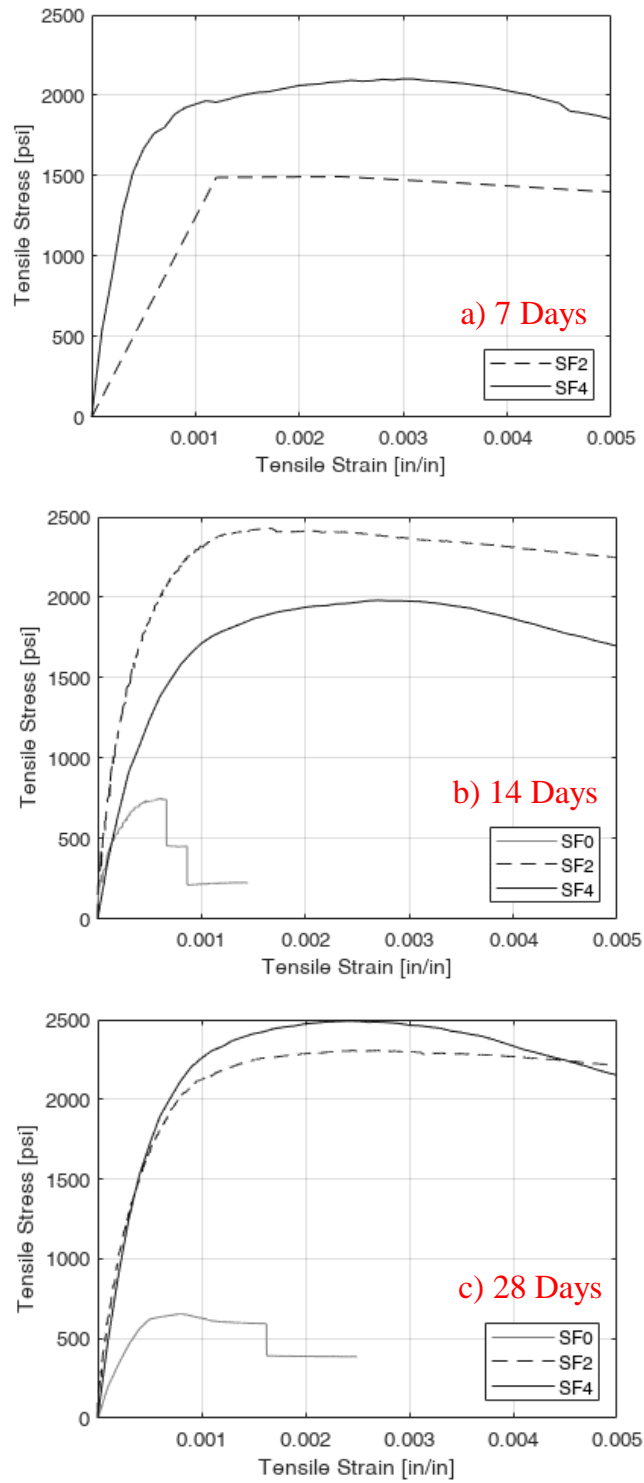
Figure 3-27 Close up view up to 0.005 strain of average tensile stress-strain relationships

for 3rd batch 1 inch dog-bone.

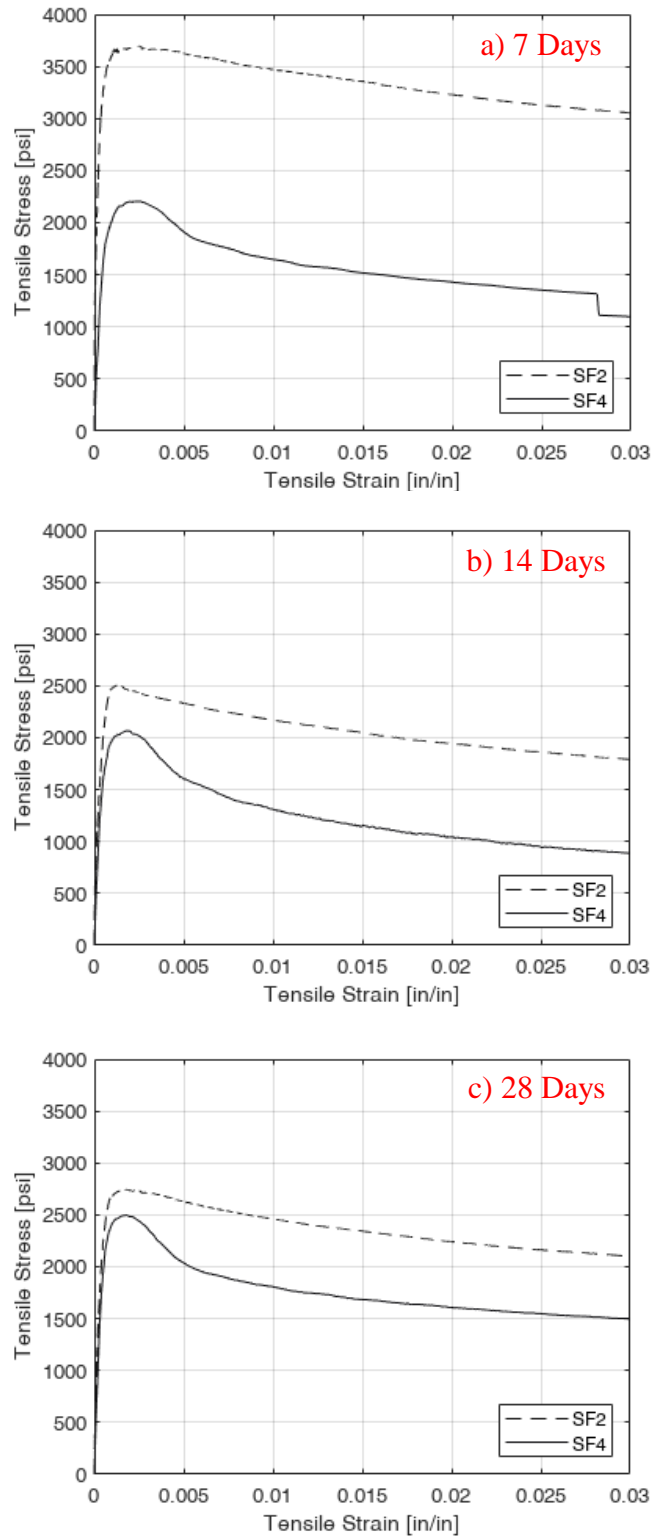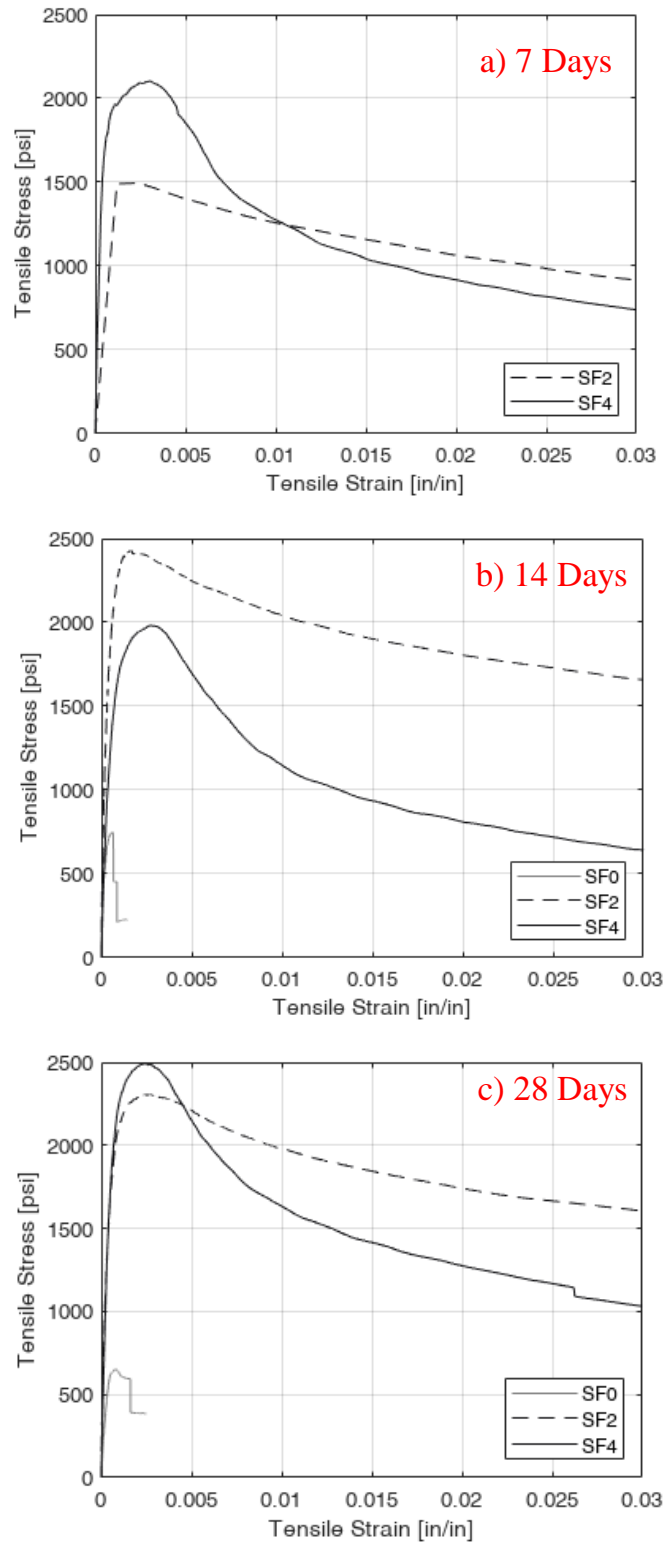Figure 3-28 Average tensile stress-strain relationships for 3rd batch 1 inch dog-bone.

4.   ASSESSMENT AND TRENDS

In this chapter all results and interpretations are discussed and highlighted. Literature's main results are briefly comparted to this studies results.

4.1 Quantitative Summary Results

4.1.1   Modulus of Elasticity

Modulus of elasticity is simply the slope of the tensile stress-strain curve, the selected two points were 10% and 30% of the specimens' average strength. Determining the specimens' elastic modulus helps in characterizing the initial behavior or the elastic phase. Elastic phase is when the relationship between stress and strain is fully linear elastic. Cracking of the specimen concludes that elastic phase. Modulus of elasticity did not vary with age or with steel fiber content, only varied with with specimen size and quality control. Table 4-6 and Table 4-7 show the 3rd batch results for dog-bones with their respective standard deviation and coefficient of variation.

4.1.2 Tensile strength

Tensile strength varied with the steel fiber and did not vary with age as it depends on the fibers and matrix combined behavior. Variations and high standard deviation were due to the random orientation of the fibers and their alignment to the cracks. Table 4-6 and Table 4-7 show the 3rd batch results for dog-bones with their respective standard deviation and coefficient of variation.

Table 4-1 Strength and averages of one inch dog-bone specimens of the 3rd batch with no

steel fiber

SF 0% Dog-bone Size A 1 Inch (ksi)					
14 Days	S1	0.79	28 Days	S1	0.71
	S2	0.68		S2	0.56
	S3	0.86		S3	0.57
	S4	0.88		S4	0.82
Average		0.8025	Average		0.665

Table 4-2 Strength and averages of one inch dog-bone specimens of the 3rd batch with

2% steel fiber content

SF 2% Dog-bone Size A 1 Inch (ksi)									
7 Days	S1	1.44	14 Days	S1	2.05	28 Days	S1	3.08	S7	2.31
	S2	1.32		S2	2.31		S2	3.01	S8	1.82
	S3	1.54		S3	2.67		S3	2.90	S9	2.71
	S4	1.55		S4	3.50		S4	1.37	S10	1.81
	S5	1.62		S5	1.77		S5	1.85	S11	1.91
	S6	1.59					S6	1.82		
Average		1.46	Average		2.46	Average				2.22

Table 4-3 Strength and averages of one inch dog-bone specimens of the 3rd batch with

4% steel fiber content

SF 4% Dog-bone Size A 1 Inch (ksi)									
7 Days	S1	2	14 Days	S1	2.76	28 Days	S1	2.45	S7	2.7
	S2	2.5		S2	1.72		S2	1.59	S8	2.9
	S3	1.85		S3	1.1		S3	2.2	S9	2.5
	S4	2.25		S4	2.7		S4	1.8	S10	3.4
				S5	1.52		S5	2.4	S11	2.67
				S6	1.87		S6	2.1		
Average		2.16	Average		2.12	Average				2.43

Table 4-4 Strength and averages of half inch dog-bone specimens of the 3rd batch with

2% steel fiber content

SF 2% Dog-bone Size B 1/2 Inch (ksi)									
7 Days	S1	2.39	14 Days	S1	3.57	28 Days	S1	2.42	S7	2.53
	S2	3.3		S2	2.23		S2	2.08		
	S3	4.7		S3	4.5		S3	3.58		
	S4	4.8		S4	4.8		S4	2.88		
	S5	4.5					S5	3.27		
	S6	5.3					S6	3.76		
Average		3.75	Average		2.9	Average				2.93

Table 4-5 Strength and averages of half inch dog-bone specimens of the 3rd batch with

4% steel fiber content

SF 4% Dog-bone Size B 1/2 Inch (ksi)									
7 Days	S1	2.72	14 Days	S1	2.05	28 Days	S1	2.68	S7	2.5
	S2	1.65		S2	2.23		S2	1.98	S8	1.73
	S3	1.73		S3	2.0		S3	2.64		
	S4	2.78		S4	1.89		S4	3.05		
	S5	1.83		S5	1.77		S5	2.42		
	S6	2.21		S6	2.63		S6	3.11		
Average		2.22	Average		2.10	Average				2.53

The following tables will show individual strength, average and standard deviation for

tensile strength of the 3rd batch dog-bone specimens.

Table 4-6 Half inch dog-bone (Size B) results.

Specimen Name	Elasticity Modulus (ksi)	Tensile Strength (ksi)	Specimen Name	Elasticity Modulus (ksi)	Tensile Strength (ksi)
	Value	Value		Value	Value
S1_SF2_B_D28	6039.8	2.43	S1_SF2_B_D28	3331.30	2.68
S1_SF2_B_D28	4069.5	2.09	S1_SF2_B_D28	2023.60	1.99
S1_SF2_B_D28	10890	3.58	S1_SF2_B_D28	2694.00	2.65
S1_SF2_B_D28	5225.4	2.88	S1_SF2_B_D28	3056.60	3.06
S1_SF2_B_D28	5206	3.27	S1_SF2_B_D28	2399.90	2.43
S1_SF2_B_D28	6146.2	3.76	S1_SF2_B_D28	3035.80	3.11
S1_SF2_B_D28	5483.3	2.53	S1_SF2_B_D28	2519.20	2.53
S1_SF2_B_D28	6260.6	1.89	S1_SF2_B_D28	1810.80	1.74
Average	6165.1	2.804	Average	2608.90	2.52
Standard Deviation	1904.24	0.64	Standard Deviation	492.83	0.45
Coefficient of variation	0.31	0.23	Coefficient of variation	0.19	0.27

Table 4-7 One inch dog-bone (Size A) results.

Specimen Name	Elasticity Modulus (ksi)	Tensile Strength (ksi)	Specimen Name	Elasticity Modulus (ksi)	Tensile Strength (ksi)
	Value	Value		Value	Value
S1_SF2_A_D28	4352.8	3.017	S1_SF4_A_D28	2412.60	2.44
S2_SF2_A_D28	3890.4	3.08	S2_SF4_A_D28	4202.20	4.23
S3_SF2_A_D28	4715.4	2.9	S3_SF4_A_D28	1646.60	1.60
S4_SF2_A_D28	4862.4	1.299	S4_SF4_A_D28	2282.80	2.18
S5_SF2_A_D28	3497.6	1.85	S5_SF4_A_D28	1751.90	1.75
S6_SF2_A_D28	3627.8	1.805	S6_SF4_A_D28	2396.60	2.39
S7_SF2_A_D28	3815.9	2.32	S7_SF4_A_D28	1998.70	2.09
S8_SF2_A_D28	3891.3	1.81	S8_SF4_A_D28	2720.50	2.72
S9_SF2_A_D28	3360.2	2.748	S9_SF4_A_D28	2915.30	2.93
S10_SF2_A_D28	3890.4	1.75	S10_SF4_A_D28	2577.40	2.53
S11_SF2_A_D28	3990.42	1.87	S11_SF4_A_D28	3545.90	3.53
			S12_SF4_A_D28	2653.30	2.66
Average	3990.42	2.22	Average	2586	2.59
Standard Deviation	452.18	0.59	Standard Deviation	691.68	0.7
Coefficient of variation	0.11	0.27	Coefficient of variation	0.27	0.27

4.1.3 Flexural strength

Flexural strength varied with steel fiber content and with age, as it depends on both compressive and tensile strength. The flexural strength test is a straightforward test, yet it incorporates some compression forces on the specimen's top section. Age is a one of the factors that affects the compressive strength and behavior. Table 4-9 show the effect of age and fiber content on the flexural strength of the modulus of rupture.

Table 4-9 Prismatic specimens' results for 4 point bending.

Modulus of Rupture (ksi) SF 0%							
7 Days	S1	0.63	14 Days	S1	0. 56	28 Days	S1	0.57
	S2	0.72		S2	0.53		S2	0.59
	S3	0.82		S3	0.65		S3	0.83
	S4	0.54		S4	0.63		S4	0.49
Average		0.68	Average		0.59	Average		0.62
Modulus of Rupture (ksi) SF 2%							
7 Days	S1	1.84	14 Days	S1	-	28 Days	S1	3.45
	S2	2.32		S2	3.4		S2	2.36
	S3	2.87		S3	2.66		S3	1.52
	S4	2.81		S4	2.02		S4	3.87
Average		2.46	Average		2.70	Average		2.80
Modulus of Rupture (ksi) SF 4%							
7 Days	S1	5.77	14 Days	S1	6.48	28 Days	S1	6.66
	S2	6.86		S2	4.68		S2	6.72
	S3	7.66		S3	7.12		S3	8.81
	S4	6.26		S4	6.26		S4	8.09
Average		6.64	Average		6.14	Average		7.57

4.2 Direct tension test size effect

As previously shown, results from ½ inch dog-bones were significantly higher than 1 inch. To add, the correlations between their tensile strength and flexural strength confirmed the unreliability of their results. Figure 4-1 shows the relation between tensile strength of Size B dog-bone with flexural strength of prismatic specimens from all three batches. R² of 0.64 is a great proof that a size effect plays a role in tensile strength and that a half inch is not suitable for capturing the true behavior. Figure 4-2a and Figure 4-2b show the correlation between tensile toughness at 0.005 and 0.01 strain, respectively and flexural toughness at 0.02 and 0.08 deflection, respectively. Figure 4-2 confirms again the unreliability of Size B dog-bones.
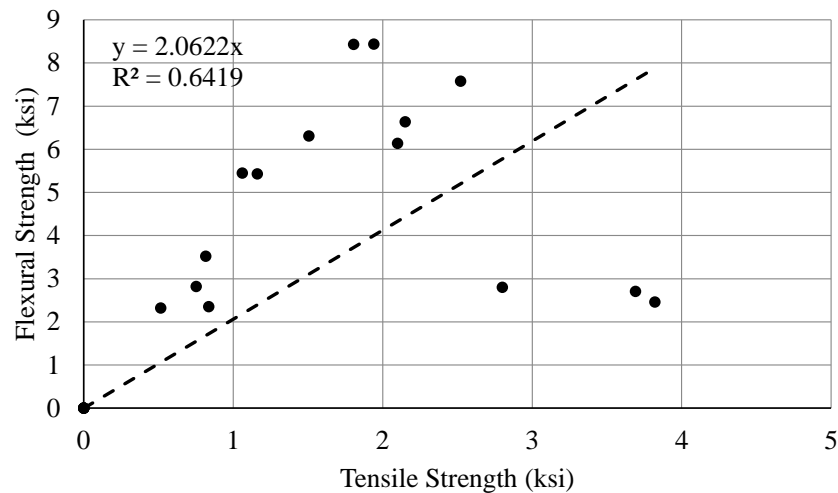

Figure 4-1 flexural strength of prismatic specimens' correlations with half inch dog-bone specimens

a) Tensile Toughness at 0.005 strain (psi.in/in)

b) Tensile Toughness at 0.01 strain (psi.in/in)
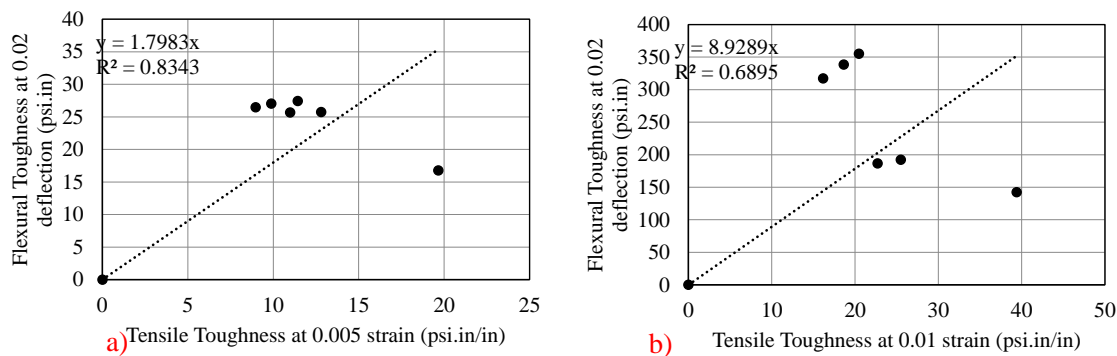
Figure 4-2 flexural toughness of prismatic specimens' relationship with tensile toughness of Size B dog-bone specimens.

4.3 Direct tensile tests: Comparison against other UHPCs

Graybeal and Baby (2019) had two prismatic specimens (S, L) with dimensions of 2 by 2 by 17 inches and 3.94 by 3.94 by 17 inches. Both sizes were tested for 4-point bending and direct tensile test. They were lab cured and tested 4 months after casting. The specimens were preloaded to a compressive load before tensile testing.

Concerning direct tensile test, Graybeal reported an average for tensile strength of 1.3 ksi, and 1.2 ksi for 2% fiber content with a standard deviation of 0.1, and 0.08. On the other hand, in this study a higher average tensile strength is reported, 2.22 ksi, and 2.74 with a standard deviation of 0.59, and 0.65 for Size A and Size B, respectively. The standard deviation in this study is higher, which can be attributed to multiple factors including curing and placing. Additionally, Graybeal reported first crack stress at 0.97 ksi, and 0.86 ksi for 2% fiber content at 0.000119, and 0.000105 strain. First crack stress achieved in this study was 2.0 ksi, and 1.3 ksi for 2% fiber content at 0.00076, and 0.00018 strain for Size A, and Size B, respectively.

Moreover, Graybeal reported an average modulus of elasticity of 8200 ksi, and 8400 ksi for 2% fiber content. While this study reported an average modulus of elasticity of 7169 ksi, and 4850 ksi for Size A, and Size B, respectively.

(Riding et al., 2022) had a nonproprietary mix of UHPC with straight and twisted steel fibers with varying steel fiber content. Their research was based on six prismatic specimens with dimensions of 2 by 2 by 17 inches for direct tensions tests and four prismatic specimens with dimensions of 4 by 4 by 14 inches for 4-point bending tests. Also, double punch test was utilized in this study using 6 by 6 inches cylindrical double punch specimens. The researchers did not mention how the specimens were cured.

For assessments, graphs were generated to compare this research results against Riding's finding. Figure 4-3 shows the the tensile results side by side with this research study's results and Riding's results.
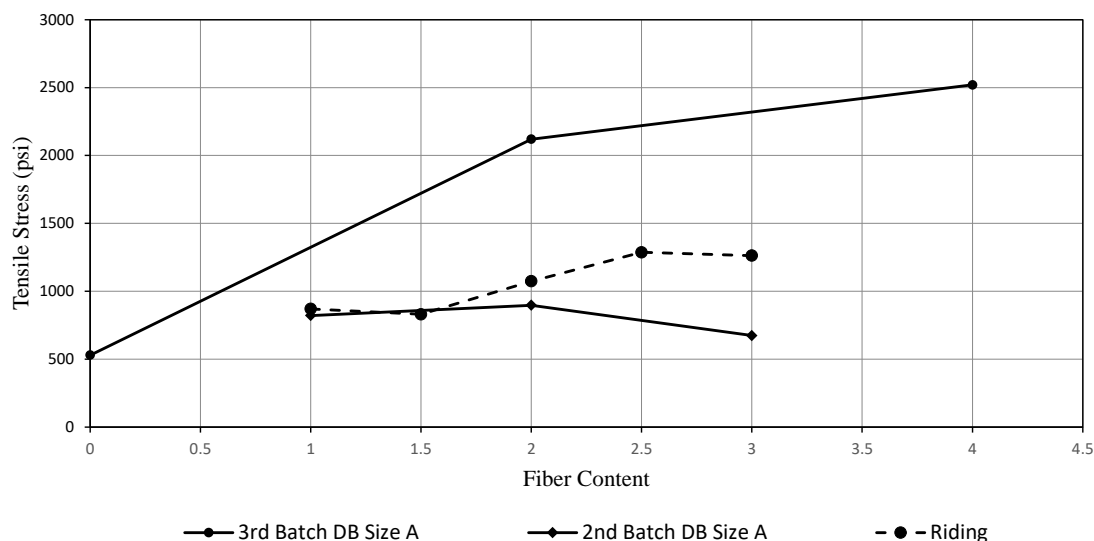

Figure 4-3 Tensile strength versus fiber content, a) work by (Riding et al., 2022) b) current research

4.4 Flexural tests Comparison against other UHPCs

Concerning 4-point bending test, (Graybeal and Baby, 2019) reported flexural strength of 2.62 ksi and 3.42 ksi for S, and L, respectively. On the other hand, in this study it is reported for the 3rd batch a flexural strength of 3.02 ksi for a 2% fiber content prismatic specimens with dimensions of 3 by 3 by 12 inches. Furthermore, Graybeal reported higher modulus of elasticity than typically encountered. For comparison, Graybeal reported a modulus of elasticity of 7322 ksi, and 7933 ksi for S, and L specimens, respectively. On the other hand, in this study, the recorded modulus of elasticity was 563 ksi for 2% steel fiber content average prismatic specimens. It should be noted that the method Graybeal followed was not fully understood so the researcher computed modulus of elasticity based on Equation(4-1).

$$\Delta x = \frac{P.a}{6.E.I} . \left(3.L.X - 3.X^2 - a^2 \right) \qquad \textit{Equation 4-1}$$

where P is load in kips, a is the distance from the point load to the support, x is the distance to the mid span from the support and I is the section inertia.

(Tadros et al.,2021) had set a target for UHPC in large study sponsored by PCI. Different UHPC mixes were tested and investigated in various ways. For the sake of the assessment in this chapter, it is focused on compressive strength, first peak (first crack) flexural strength, peak (ultimate) flexural strength, ratio of peak (ultimate) flexural strength to first peak (first crack) flexural strength, and residual strength at net mid-span deflection of L/150 (Tadros et al., 2021).

Table 4-11 Target for UHPC Set by (Tadros et al., 2021)

Property	Test Method	Performance Target
Flow spread	ASTM C1856	8 to 10 inches, measured not longer than 15 minutes before placement
Compressive strength	ASTM C1856	≥ 10.00 at prestress release ≥ 17.40 ksi at service
first-peak (first crack) flexural strength, f_l	ASTM C1856	≥ 1.500 ksi at service
peak (ultimate) flexural strength, f_p	ASTM C1856	≥ 2.000 ksi at service
Ratio of Peak (ultimate) flexural strength, f_p to First-peak (first crack) flexural strength, f_l	ASTM C1856	≥ 1.25 at service
Residual flexural strength at net mid-span deflection of L/150	ASTM C1856	≥ 75% of first-peak (first-crack) strength at service

Tadros et al. (2021) focused on UHPC with 2% steel fiber content and had various mixtures. In this study we will compare and check if the tested material in this research study passed their target and if not, where did it fail. For compressive strength, the material achieved around 20 ksi at 28 days (Cimesa & Moustafa, 2022). For first flexural crack on average, the third batch reached to 2.7 ksi while the first batch reached to 1.9 ksi for 2% steel fiber content. Peak flexural strength for 2% fiber content was 3.0 ksi for the third batch and 5.0 ksi for the first batch. Ratio of peak flexural strength to first crack was 1.1 for the third batch and 2.5 for the first batch. Last property was the residual flexural strength at mid span at span deflection of $L/150$, it was 3.0 ksi and 3.9 ksi for the first batch which corresponds to 85%, and 190% for the third and first batch, respectively.

That concludes the assessment that Tadros had set, the material outperformed the target with a large margin except for the ratio of peak flexural strength to first peak (first crack) flexural strength, as the third batch failed by 0.15%.

(Akça & İpek, 2022) focused on optimizing a nonproprietary mix of UHPC and they tested their specimens under 3 point bending. They had their specimens either water tank cured or using a wet cloth. They tested prismatic specimens with dimensions of 3.9 by 3.9 by 15.74 inches for 4-point bending test and 1.96 by 1.96 by 11.81 inches for direct tensile test. They implemented a hybrid and straight steel fiber mixes with either 2% or 3% fiber content. Their final mix reached 2700 psi for flexural strength and 65 psi.in for toughness at deflection of 1.1 inches for a straight steel fiber content of 2%. On the other hand, for similar mix in this study, a flexural strength of 2800 psi was reached and a toughness of 276 psi.in at deflection of 1.1 inches was achieved.

Riding's research for flexural testing was concluded on prismatic specimens with dimensions of 4 by 4 by 14 inches for 4-point bending tests. For assessment, graphs were generated to compare this research results against Riding's finding.
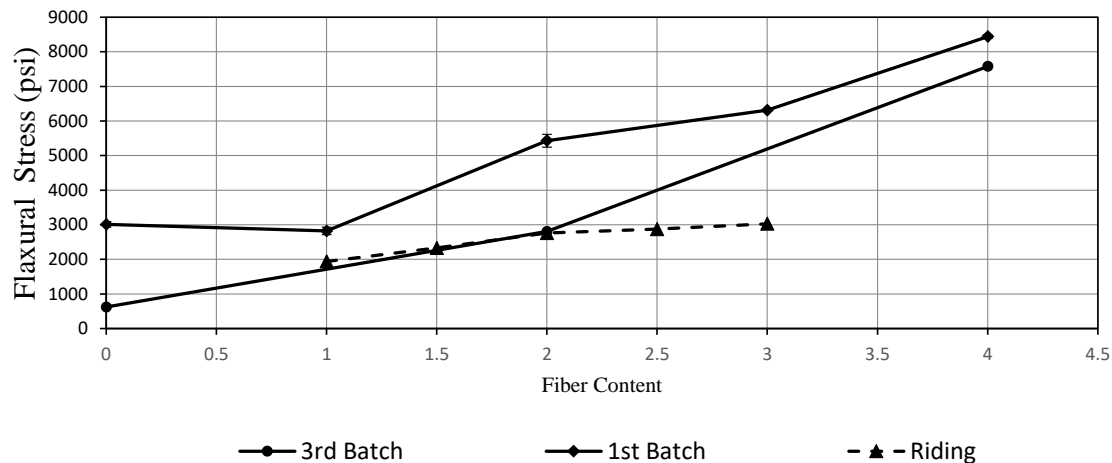
Figure 4-4 Modulus of Rupture and fiber content relationship a) work by (Riding et al.,

2022) b) current research

Another relationship that highlights the behavior of UHPC is flexural toughness at certain

strain, which allows the research community to compare behaviors and form an idea on the

ductility of the material. Figure 4-5 and Figure 4-6 show flexural stress at $L/150$ and $L/600$

deflection, respectively.
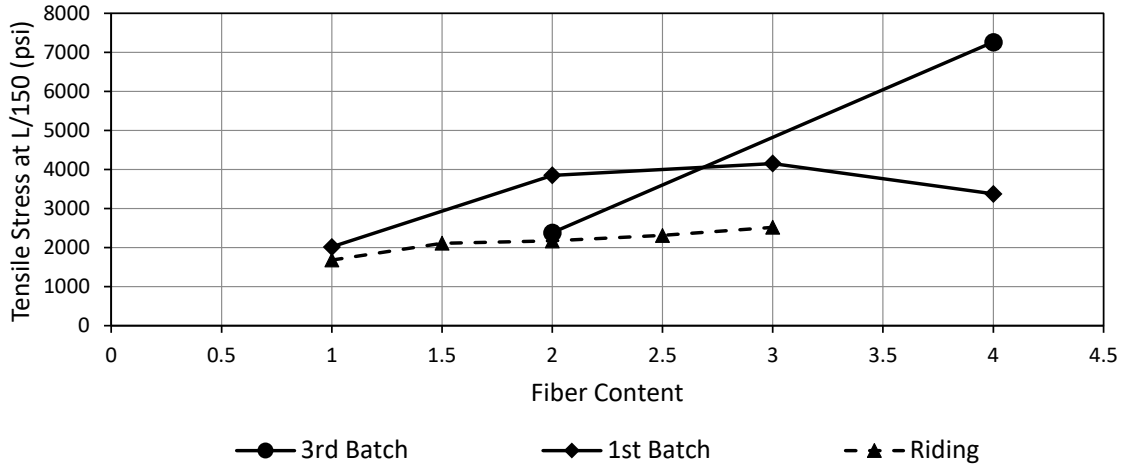
Figure 4-6 Flexural stress at deflection of L/150 a) work by (Riding et al., 2022) b)

current research
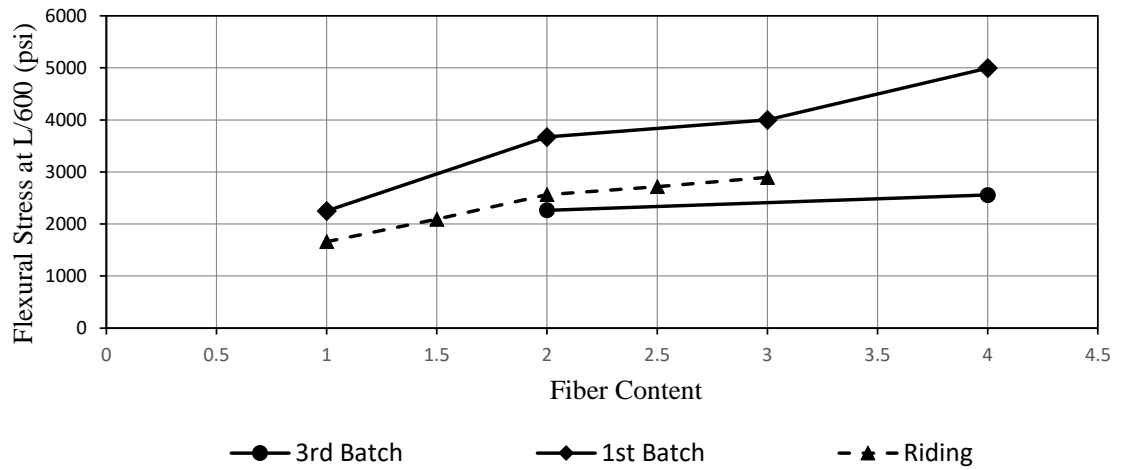
Figure 4-7 Flexural stress at deflection of L/600.

4.5 Flexural vs direct tension results

Additionally, Riding corelated toughness for flexural bending and direct tensile testing. It indicated a good correlation. Similar conclusions were reached in this study as shown in Figure 4-7. It is a good indicator or criteria to assess UHPC. Toughness or area under the curve demonstrates how resilient a material can be with holding load for a sustained amount of strain or deflection. Figure 4-8a and Figure 4-8b show an R^2 value of higher than 0.8, indicating a strong correlation between prismatic specimens and Size A dog-bone.
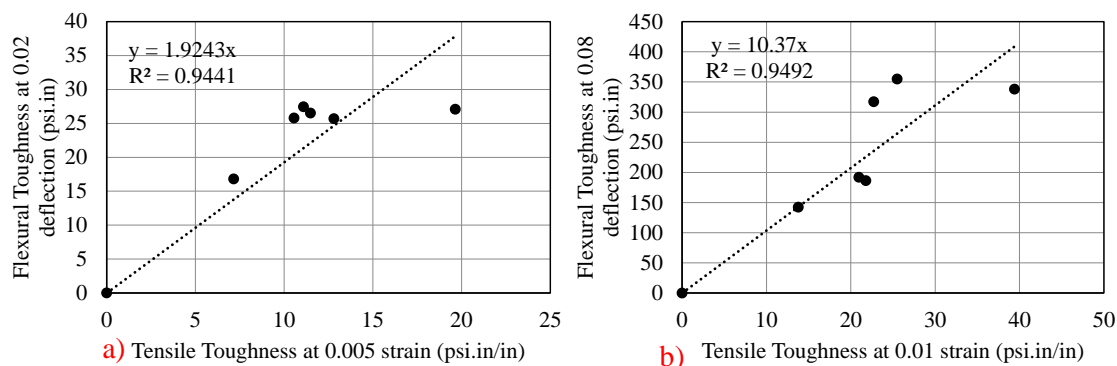
Figure 4-8 Correlation between flexural and tensile toughness

Furthermore, another great correlation was found, Figure 4-9 shows an acceptable R^2 value for the relation between flexural strength and tensile strength.
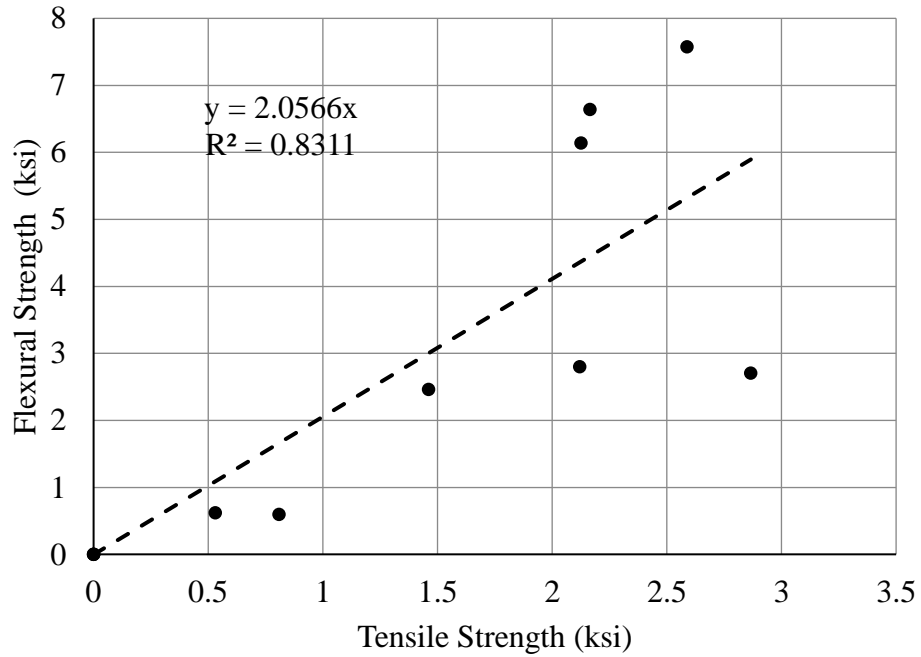
Figure 4-9 Correlation between flexural strength and tensile strength.

From the reported results, we can conclude that a higher strength was found to the tested material in this study despite the different dimensions and conditions. Yet, we had significant higher standard deviation and disperse results.

5.   OUTCOMES, CONCLUSION AND RECOMMENDATIONS

The thesis presented four chapters that summaries the work of one research student over 3 semesters. The following subsections condenses the summary and outcomes of this research study. All details can be found in the chapters. Nonetheless for an overall summary, key findings, and recommendation for future work are provided in this chapter.

5.1 Outcomes

The comprehensive goal of this research study is to lay the ground for characterization of tensile behavior of Carbon Nanofiber enhanced UHPC. The study has successfully provided readily available full family full stress strain/deflection curves of the material. They can be used for future research work or design purposes. Carbon Nanofibers did not improve elastic modulus or effect it. Nevertheless, they had a positive impact and enhancement on tensile strength and strain capacity compared to traditional UHPC. There is a sweet spot for implementing steel fibers and getting the most benefit of implementing them. Ideally, that spot is from 2% to 3% fiber content. Any addition of steel fibers more than 3% will not have a similar gain of strength to the increasing the fiber content from 2% to 3% or 1% to 2%, also it will have an adverse effect on the strain capacity. Addition of steel fibers to specimens by 1% volume leads to 120% increase in strength, while increasing from 1% to 2% will result into 80% increase in strength. While increasing fiber content from 2% to 3% will result into 30% increase in strength. Yet increasing the fiber content from 3% to 4% will only result in an increase of strength by 15%.

There is no consensus on the methods to characterize a tensile behavior for concrete. The research community at large did not agree on a testing method, curing, specimen dimensions or even a criteria for assessing. Although, the ASHTO proposed the 2 by 2 inch specimen for direct tensile test, it was met with resistance as most research labs do not have the capabilities to test the proposed specimen size. However, ACI community suggested that the proposed specimen would be used as a one-time test and be correlated to from the 4 point bending test, meaning that future research would be a limited to a set of 28 days specimen of the proposed dimension tested for direct tensile and then followed by a large set of prismatic specimens tested for 4 point bending test.

For these reasons, the researcher could not properly conduct a proper comparison between this research and the literature.

5.2 Key Conclusions

The following key conclusions were drawn based on the findings, observations, and data of different areas of this research.

- Full tensile behavior of carbon nanofibers UHPC has been characterized herein and full stress-strain relationships are provided for future modeling and design. However, further research is still needed to account for different materials variability, varying nanofibers ratio, and other curing and placing techniques.

- Strength should not be the only sought factor for UHPC, toughness at a certain strain or deflections value are great and simple indictors for resilience and ductility of UHPC.

- Based on the correlations and results, the four-point bending test is the most reliable testing method to evaluate a material and is recommended, but it is not sufficient to fully characterize tensile behavior and direct tension tests would be still needed.

- Size effect is important to account for and study when testing for tensile behavior.

5.3 Recommendations for Future Work

Giving the emerging nature of UHPC types, testing methods and specifications, and applications, the following are few points for future studies to consider:

- Apply the upcoming AASHTO tensile test specification, which requires 2 by 2 inch specimen for direct tensile testing, for Carbon Nanofibers UHPC and characterize the behavior accordingly.

- Carbon Nanofibers UHPC future research should consider larger applications and full scale structural elements with traditional reinforcement.

- While full scale columns with Carbon Nanofibers enhanced UHPC are being investigated in UNR, the effect on nanofibers on confinement and axial stiffness is yet to be explored in more details.

- Flexural behavior Carbon Nanofibers is promising, and as such, full-scale bridge girders and slabs could be good applications and should be investigated.

6. REFERENCES

1. Abokifa, M., M.A. Moustafa, (2021). "Experimental Behavior of Precast Bridge Deck Systems with Non-Proprietary UHPC Transverse Field Joints", Materials, 14 (22), 6964

2. Abokifa, M., M.A. Moustafa, (2021). "Full-Scale testing of Non-Proprietary Ultra-High Performance Concrete for Deck Bulb Tee Longitudinal Field Joints", Engineering Structures, 243, 112696

3. Abokifa, M., M.A. Moustafa, (2021). "Mechanical Characterization and Material Variability Effects of Emerging Non-Proprietary UHPC Mixes for Accelerated Bridge Construction Field Joints", Construction and Building Materials, 308, 125064

4. Aboukifa, M., M.A. Moustafa, (2021). "Experimental Seismic Behavior of Ultra-High Performance Concrete Columns with High Strength Steel Reinforcement", Engineering Structures, 232, 111885

5. Aboukifa, M., M.A. Moustafa, (2022). "Reinforcement Detailing Effects on Axial Behavior of Full-Scale UHPC Columns", Journal of Building Engineering, 49, 104064

6. Aboukifa, M., M.A. Moustafa, (2022). "Structural and Buckling Behavior of Full-Scale Slender UHPC Columns", Engineering Structures, 255, 113928

7. Aboukifa, M., M.A. Moustafa, A. Itani. (2020). "Comparative Structural Response of UHPC and Normal Strength Concrete Columns under Combined Axial and Lateral Cyclic Loading", ACI Special Publication, 341, p. 71-96

8. Aboukifa, M., M.A. Moustafa, M.S. Saiidi, (2021). "Seismic Response of Precast Bridge Columns with Composite Non-Proprietary UHPC Filled Ducts ABC Connections", Composite Structures, 274, 114376

9. Akça K. R., İpek M., (2022) Effect of different fiber combinations and optimization of an ultra-high performance concrete (UHPC) mix applicable in structural elements, Construction and Building Materials, (Vol. 315).

10. Akeed M. H., Qaidi S., Ahmed H. U.,Faraj R. H. ,Mohammed A.S. , Emad W., Tayeh B. A., Azevedo A. R.G. (2022) Ultra-high-performance fiber-reinforced concrete. Part I: Developments, principles, raw materials, Case Studies in Construction Materials, (Vol. 17).

11. ASTM C1609/C1609M − 19a. (2019). "Standard Test Method forFlexural Performance of Fiber-Reinforced Concrete (Using Beam With Third-Point Loading).

12. Cimesa, M., M.A. Moustafa (2022). "Experimental characterization ad analytical assessment of compressive behavior of carbon nanofibers enhanced UHPC", Case Studies in Construction Materials, 17, e01487

13. Dhakal, S., M.A. Moustafa, (2019). "MC-BAM: Moment-Curvature Analysis for Beams with Advanced Materials", SoftwareX, Volume 9, pp. 175-182

14. Fan D., Yu R., Shui Z., Liu K., Feng Y., Wang S., Li K., Tan J., He Y. (2021). A new development of eco-friendly Ultra-High performance concrete (UHPC): Towards efficient steel slag application and multi-objective optimization, Construction and Building Materials, (Vol. 306).

15. Gagg C. R., Cement and concrete as an engineering material: An historic appraisal and case study analysis, Engineering Failure Analysis, (Vol. 40, 114-140).

16. Gay C., Sanchez F. (2010). Performance of Carbon Nanofiber-Cement Composites with a High-Range Water Reducer. Transportation Research Record.

17. Graybeal B., Tanesi J. (2007). Durability of an Ultra high-Performance Concrete. Journal of Materials in Civil Engineering.

18. Haber Z. B., De La Varga I., Graybeal B. A., Nakashoji B., El Helou R., Properties and Behavior of UHPC-Class Materials, FHWA-HRT-18-036.

19. HI-CON (website). Retrieved from https://www.hi-con.com/products/facades-in-uhpc/.

20. Huang, K., Xie, J., Wang, R., Feng, Y. & Rao, R. (2021). Effects of the combined usage of nanomaterials and steel fibers on the workability, compressive strength, and microstructure of ultra-high performance concrete. Nanotechnology Reviews, 10(1), 304-317.

21. Isa M.N., Pilakoutas K., Guadagnini M. (2021). Determination of tensile characteristics and design of eco-efficient UHPC, Structures, (Vol. 32, 2174-2194).

22. Joe, C.D. and M. A. Moustafa*, (2016) "Cost and Ecological Feasibility of Using UHPC in Bridge Piers," First International Interactive Symposium on UHPC, Des Moines, IA, USA, July 18-20, 2016.

23. Li J., Wu Z., Shi C., Yuan Q., Zhang Z. (2020) Durability of ultra-high performance concrete – A review, Construction and Building Materials, (Vol.255).

24. Meng W., Khayat K. H., (2018). Effect of graphite nanoplatelets and carbon nanofibers on rheology, hydration, shrinkage, mechanical properties, and microstructure of UHPC, Cement and Concrete Research, (Vol. 105, 64-71).

25. Metaxa Z. S., Konsta-Gdoutos M. S., Shah S. P. (2010). Carbon Nanofiber-Reinforced Cement-Based Materials. (Vol. 2142-1).

26. Muhd Norhasri M.S., & Hamidah M.S., & Fadzil A.M. (2019). Inclusion of nano metaclayed as additive in ultra-high performance concrete (UHPC), Construction and Building Materials, (Vol. 201,590-598).

27. Naeimi, N., M.A. Moustafa, (2020). "Numerical Modeling and Design Sensitivity of Structural and Seismic Behavior of UHPC Bridge Piers", Engineering Structures, 219, 110792

28. Naeimi, N., M.A. Moustafa, (2021). "Analytical Stress-Strain Model for Steel-Spiral Confined UHPC", Composites Part C: Open Access, 5, 100130

29. Naeimi, N., M.A. Moustafa, (2021). "Compressive Behavior and Stress-Strain Relationships of Confined and Unconfined UHPC", Construction and Building Materials, 272, 121844

30. Park S.H. , Kim D. J., Ryu G. S., Koh K. T. (2012). Tensile behavior of Ultra High Performance Hybrid Fiber Reinforced Concrete, Cement and Concrete Composites, (Vol. 34, Issue 2).

31. Qiu M., Zhang Y., Qu S., Zhu Y., Shao X. (2020) Effect of reinforcement ratio, fiber orientation, and fiber chemical treatment on the direct tension behavior of rebar reinforced UHPC, Construction and Building Materials, (Vol. 256).

32. Ridding K. A., Ferraro C. C., Hamilton T., Harely J., Alrashidi R., Voss M. S. (2022). Comparison between Direct Tension, Four-Point Flexure, and Simplified Double Punch Tests for UHPC Tensile Behavior.

33. Safiuddin, Md, Gonzalez M., Cao J., Tighe S. (2013). State-of-the-art report on use of nano-materials in concrete. International Journal of Pavement Engineering.

34. Tadros M., Lawler J., Abo El Khier M., Kurt A., Wagner E., Gee D., Lucier G. (2021). Implementation of Ultra-High Performance Concrete in Long Span Precast Pretensioned Elements for Concrete Buildings and Bridges.

35. Yirui Li Y., Xiaohui Zeng X., Ye Shi Y., Kai Yang K., John Zhou J., Hussaini Abdullahi Umar H., Guangcheng Long G., Youjun Xie Y. (2022). A comparative study on mechanical properties and environmental impact of UHPC with belite cement and portland cement, Journal of Cleaner Production, (Vol. 380, Part 1).

36. Yu R., Spiesz P., Brouwers H.J.H. (2014). Effect of nano-silica on the hydration and microstructure development of Ultra-High Performance Concrete (UHPC) with a low binder amount, Construction and Building Materials, (Vol. 65, 140-150).